ELUCIDATION OF THE C-DI-GMP MEDIATED SIGNALING MECHANISM IN A BACTERIAL TRANSMEMBRANE RECEPTOR

A Thesis

Presented to the Faculty of the Graduate School

of Cornell University

In Partial Fulfillment of the Requirements for the Degree of

Master of Science

by

Maithili Sudhir Deshpande

August 2019

ABSTRACT

The LapA/LapG/LapD system is a common biofilm effector system found in over 1000 bacterial genomes and is mediated by the bacterial second messenger, cyclic-di-GMP or c-di-GMP. C-di-GMP along with the proteins that synthesize it (diguanylate cyclases or DGCs with GGDEF domains) and degrade it (phosphodiesterases or PDEs with EAL or HD-GYP domains) are important regulators of biofilm formation. Although some aspects of the biofilm formation process are fairly well understood, much still remains to be elucidated at the molecular level, especially the signaling mechanisms and the associated conformational changes in these proteins that are crucial for cell adhesion in a wide variety of bacteria, including several human pathogens. This study was undertaken to fill some of these gaps in our knowledge, focusing on the molecular mechanism of the transmembrane c-di-GMP receptor LapD, the main signaling switch in this pathway in *Pseudomonas fluorescens*.

In this study, we introduced single amino acid cysteine mutations spanning the entire HAMP domain and the S-helix in a LapD-green fluorescent protein-fusion protein. As LapD exists as a homodimer as its smallest functional unit, a single amino acid substitution is represented once in each monomeric unit and the intra-dimer crosslinking of these residues was reported. Four distinct states/conformations of LapD were studied: 1) apo, 2) in the presence of c-di-GMP, 3) in the presence of LapG, and 4) in the presence of both c-di-GMP and LapG. Cysteine crosslinking experiments were performed on these four states of LapD by mildly oxidizing the

protein in the presence of the catalyst copper phenanthroline [$Cu(Phen)_2$]. The presence of disulfide dimer formation was detected using in-gel fluorescence by monitoring electrophoretic mobility shifts of the msfGFP-fusion protein on SDS-PAGE gels.

Most of the 68-cysteine mutants generated spanning the HAMP domain and the S-helix displayed a significant level of intra-dimer crosslinking irrespective of whether they were proximally or distally located in the helices, or whether they were buried or surface-exposed. LapD thus appears to exist in multiple conformations in solution such that even more distal residues in the helices could come into close contact with each other. Periplasmic domain mutants located closer to the LapG binding site showed the highest levels of crosslinking for the partially activated LapG-LapD bound protein. Less crosslinking was observed whenever c-di-GMP was also available for binding. However, mutants located closer to the transmembrane domain showed higher crosslinking rates in the presence of c-di-GMP.

Cysteine substitutions made on helix α1-H crosslinked readily in the absence of oxidant, whereas residues on helix α2-H showed little crosslinking under similar experimental conditions. In partially and fully activated states of LapD, consecutive residues on α2-H helix showed large differences in disulfide bond formation, whereas it tended to be similar for residues belonging to the α1-H. Cysteine mutations in residues located on α2-H also revealed the presence of an additional cross-linked species in conditions where LapD was able to form dimer-of-dimers.

The fact that crosslinks were observed in different states of LapD activation and that the rates of disulfide bond formation differed across different activation states

implies that LapD may operate by oscillating between different bundle conformations. Our results, therefore, suggest that LapD's signaling mechanism appears to be more consistent with a dynamic bundle model rather than a conventional two-state signaling model such as the gearbox model.

BIOGRAPHICAL SKETCH

The author was born in California, U.S.A. in 1995. After a brief schooling in the U.S., she moved to India with her parents and completed her high school education in Delhi Public School, Hyderabad. She joined the National Institute of Technology, Surathkal (NITK), India, in 2013 to pursue her undergraduate degree in Chemical Engineering. After graduating in 2017, she joined Cornell University for her master's degree in chemical and biomolecular engineering and carried out independent research in elucidating conformational changes in a bacterial transmembrane receptor.

Dedicated to the memory of Prof. S.K. Sathe

who first introduced me to the wonderful world of protein chemistry

ACKNOWLEDGEMENTS

It is a great pleasure to express my gratitude to Prof. Holger Sondermann for his guidance, encouragement and the immense support he provided during the course of this study. I am grateful to him for taking on a student from a different field with limited knowledge in biochemistry and biology. Holger has been extremely patient and approachable over the two years I spent in his lab and his guidance has been instrumental in helping me become a better researcher. I would also like to thank my committee member, Dr. Susan Daniel for her advice and inputs.

Sincere appreciation is extended to all the lab members for their kindness and assistance and for making me feel comfortable in the lab. I would like to thank Justin Lormand for all his help in teaching me the theory and the various techniques involved in my research. His monumental patience in answering and clarifying my million doubts and questions regardless of the time is immensely appreciated. My heartfelt thanks to Carolyn Kelly for her encouragement and help, and for generously sharing her expertise and experiences during my stay in the lab. Sincere appreciation is also extended to Maria Font for her boundless energy, amazingly cheerful nature and for all her help in the lab.

I would like to acknowledge Dr. Peter Borbat, the Freed Lab and the National Biomedical Center for Advanced Electron Spin Resonance Technology (ACERT) for all the help with my ESR experiments. Sincere appreciation is also extended to Dr. Rick Cooley for initiating and optimizing the protocols for the crosslinking project and to Karin Eger for generating some of the mutants used in this study.

I would like to thank my friends Yash and Kritika for all the support they provided and for always being there to fall back on. Without them, my transition to living in Ithaca and being a master's student here would have been extremely difficult.

I am immensely grateful to my family for all the love and endless support they have provided over the years, their constant encouragement and for giving me an opportunity to carry out my graduate studies at Cornell University.

Finally, I would like to acknowledge late Dr. Shridhar Sathe, Florida State University, for all the guidance he had provided to me over the last few years, for introducing me to the field of protein chemistry and helping me realize that this was what I wanted to do. I will fondly cherish your memories and teachings forever.

TABLE OF CONTENTS

LIST OF FIGURES

LIST OF TABLES

CHAPTER 1

BIOFILMS: A LITERATURE REVIEW

The important discoveries of Robert Hooke who laid the foundations of cell theory and Anton van Leeuwenhoek who first observed and described living microbes using a homemade microscope in the 17th century opened the floodgates into the until then invisible world of microorganisms (Costerton et al., 1999; Tolker-Nielsen, 2014; Rabin et al., 2015). The field made rapid strides in the 19th century with the work of Louis Pasteur, who demonstrated that microorganisms are everywhere and provided the impetus for the development of aseptic techniques in the laboratory and the early foundations for the germ theory of disease. Subsequently, Robert Koch's research provided further support for this theory. Koch's postulates are still used for demonstrating that a specific microorganism transmits a specific disease (Evans, 1978; Lappin-Scott et al., 2014). Rapid advances in instrumentation, biochemistry, cell and molecular biology, genetic engineering and biotechnology in the 20th century have opened new avenues in understanding both the beneficial as well as adverse effects of microbes. These discoveries have shed light on how microbes affect our daily lives, and how they have extensively contributed to the development of the earth's habitats and the evolution of other life forms. (Donlan, 2002; Hoiby, 2017).

Even though van Leeuwenhoek first observed microorganisms on tooth surfaces and can be credited with the discovery of microbial biofilms (Costerton et al., 1999), microorganisms were largely considered as single, free-floating ('planktonic') cells. Using the planktonic cell culture model in nutritionally rich culture media, scientists were able to study several deadly bacterial pathogens and developed novel

ways to kill them (Donlan, 2002; Rabin et al., 2015). However, the realization of the extent to which microbial growth and development occurs on both biotic and abiotic surfaces has happened quite slowly. Henrici (1933) first reported that aquatic bacteria were not free-floating organisms, but grew on submerged surfaces. Soon thereafter, Heukelekian and Heller (1940) described how colonial growth attached to surfaces produced bacterial slime. Zobel (1943) also reported that bacteria were more commonly found attached to solid surfaces and only a small fraction existed as single, suspended cells in natural aquatic systems.

By early 1970s, Characklis (1973) reported that microbial slimes in industrial water systems were quite resistant to disinfectants such as chlorine and were difficult to remove. Clinically, the importance of biofilms was first realized in 1977 when *Pseudomonas aeruginosa* aggregation was found in sputum from the lungs of infected cystic fibrosis patients (Hoiby et al., 1977). Costerton et al. (1978) extensively studied the presence of biofilms in dental plaque and rocky mountain streams and first coined the term "biofilm". They proposed mechanisms whereby microorganisms adhere to biotic and abiotic surfaces, and mentioned their ecological significance. Since then with the advent of specific molecular fluorescent stains, high-resolution three-dimensional imaging techniques (*i.e.* confocal laser scanning microscopy), molecular-reporter technology and biofilm-culturing apparatus, it became quite evident that biofilms are not just passive aggregation of bacterial cells that are stuck to surfaces, but are structurally and dynamically complex biological systems (Hall-Stoodley et al., 2004). Current research on the genes involved in bacterial cell adhesion and biofilm formation and regulation has greatly improved our understanding of this process in

identifying targets or processes to develop novel drug therapies to prevent bacterial biofilm formation (Rabin et al., 2015; Tolker-Nielsen, 2014).

1.1. What Are Biofilms?

Microorganisms (bacteria, fungi, yeasts, molds, viruses) are primarily found in two forms: either free-floating in water (planktonic), or attached to a biotic or abiotic surface (sessile) where they congregate in large numbers to form a film or slime layer known as a "biofilm." Historically, microbiologists have focused on the results of empirical research work on planktonic cells growing in suspension in a liquid growth medium. It is now widely acknowledged that a majority of microbial cells live in spatially distinct communities or biofilms. Their behavior in biofilms is also quite different than that in planktonic state. It has been estimated that 99% of all bacteria exist in biofilms, with only 1% living in the free-floating planktonic state (Paraje, 2011).

Costerton, recognized as the founding father of the field of biofilms, defined microbial biofilms as "populations of microorganisms that are concentrated at an interface (usually solid-liquid) and typically surrounded by an extracellular polymeric substance (EPS) matrix" (Costerton, 2007; Hall-Stoodley et al., 2004). Aggregates of cells not attached to a surface are sometimes termed "flocs" and have many of the same characteristics as biofilms. A visual representation of a *P. aeruginosa* biofilm is shown in Figure 1.1.

Microorganisms in biofilms often display some characteristic features that are not shared with the same microorganisms in the planktonic state. The cells in biofilms are embedded in the EPS matrix that is at least partially composed of polymers

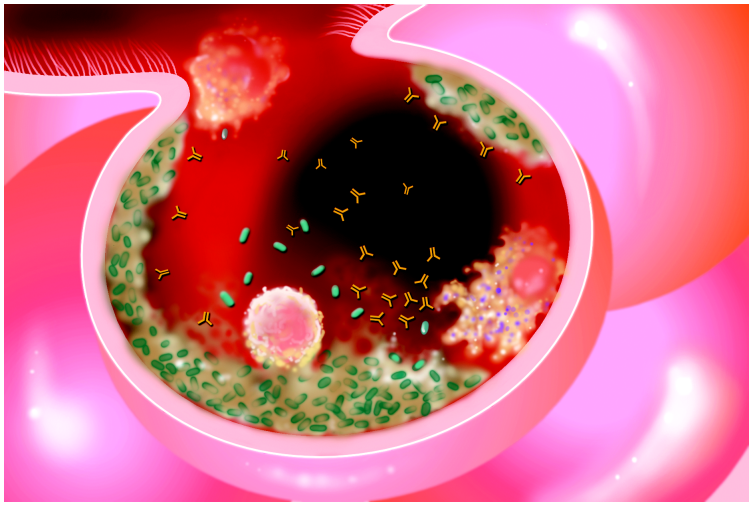

Figure 1.1. Visual representation of *Pseudomonas aeruginosa* biofilm in lung alveolus

When the immune response is compromised, bacteria are able to colonize the tiny alveoli sacs of the lungs to form biofilms. Biofilms do not trigger the neutrophils to become activated, even in the presence of antibodies (yellow Y-shaped symbols). A well-established biofilm will grow thicker over time and may calcify, thus rendering the alveoli inactive.

Courtesy: National Science Foundation

produced by the microorganisms themselves. They also display an altered phenotype with respect to gene expression, protein production, and growth (Donlan, 2002). Biofilms may also contain mixed populations of bacteria, fungi, and protozoa. Biofilms thus represent a very complex form of microbial life that is primarily characterized by a more or less immobilized lifestyle. This mode of survival and growth is also fundamental to the ecology and biology of microorganisms and allows for a protected mode of growth and survival in a hostile environment. These sessile biofilm communities also give rise to non-sessile, planktonic bacteria that can rapidly multiply and disperse.

Microbial heterogeneity is another characteristic feature of biofilms. Aerobic microorganisms in a biofilm consume oxygen, thereby creating an anaerobic zone in the interior portions of the biofilm (Flemming, 1998). This provides habitats for anaerobic microorganisms that otherwise would not grow and proliferate under aerobic conditions. A few others may use the byproducts of another microbial species as nutrients for their own activities. Therefore, biofilms in nature are made up of several different species of microorganisms and consist of several different microenvironments suitable for specific organisms and microbial activity.

This synergism or symbiotic relationship also allows protection against fluctuating environmental conditions (e.g., pH, nutrients, shear forces), disinfectants, antibiotics, and host immune responses (Jefferson, 2004). All microorganisms within biofilms thus live symbiotically together and depend on other microorganisms for energy, carbon, and other nutrients. In such structured communities, bacteria can be 1000-fold more resistant to antimicrobials than their planktonic counterparts (Mah and

O'Toole, 2001). It is now widely recognized that many commercially available biocides as well as conventional antibiotics are ineffective against biofilms and, at best, merely control planktonic microorganisms. Biofilms remain intact to continue to re-contaminate and build resistance against antimicrobial compounds. The establishment, maintenance and existence of biofilm communities are thus highly complex, socially organized processes (Mah and O'Toole, 2001).

1.2. Habitat of Biofilms

Biofilms can form on a wide variety of wet surfaces in most ecosystems in nature where nutrients are available. These include, among others, human tissues (e.g., lungs and skin), medical devices (e.g., urinary catheters), natural aquatic systems, and industrial equipment and pipelines. Its thickness varies from a single cell layer to a large community of cells sufficiently thick to be visible to the naked eye. Prakash et al. (2003) have defined aqueous biofilms as "highly complex systems containing non-cellular materials such as mineral crystals, corrosion particles, clay or silt particles, freshwater diatoms and filamentous bacteria." In contrast, the biofilms on medical devices are usually composed of a single, coccoid organism or blood components. The ability of microorganisms to become sessile by binding to various surfaces is ubiquitous in diverse ecosystems. It offers a strong survival or selective advantage for surface dwellers over their free-floating planktonic counterparts.

Biofilms are generally more abundant, densely packed and thicker in environments where nutrient availability is quite high (Prakash et al, 2003). High nutrient concentrations promote the transition of bacterial cells from the planktonic to the sessile state, while a depletion of the nutrient levels often causes detachment of

biofilm cells from surfaces (O'Toole et al., 2000; Rochex and Lebeault, 2007). Temperature, surface (whether rough or smooth), velocity and turbulence and hydrodynamics are some of the other factors that can affect the biofilm formation (Melo and Bott, 1997; Prakash et al., 2003; Donlan, 2002).

1.3. Composition of Biofilms

A typical biofilm is primarily composed of water, microbial cells, extracellular polymeric substances (EPS) that contribute 85-98% of the organic matter, microbial cells, occluded organic and inorganic particles, substances adsorbed to EPS, and those dissolved in the interstitial water. Biofilms also contain channels in which water, air and nutrients can circulate. Gradients of chemicals and ions between micro-zones provide the power to shunt the nutrients around the biofilms (Paraje, 2011). Microorganisms in the biofilms are embedded in the EPS. The extracellular substances are mostly polymers of complex polysaccharides, proteins and glycopeptides, lipids, lipopolysaccharides and other substances. They serve as a scaffold and hold the biofilm together (Flemming and Wingender, 2010). The inherently high heterogeneity of EPS among different bacterial cells makes it difficult to elucidate its specific role(s) in biofilms. The EPS, however, is known to impact structural stability, attachment, protection and infectivity of biofilms (Danese et al., 2000; Hentzer et al., 2001). Wingender et al. (1999) reported that interactions between proteins via multivalent cations are more dominant than those between polysaccharides and proteins, although the presence of non-covalent (*i.e.*, London forces, electrostatic interactions and hydrogen bonding) as well as hydrophobic interactions also plays an important role within the biofilm matrix and improve its

stability. The resistance of biofilms to several biocides and antibiotics can at least partially be attributed to the EPS. It acts as a protective coating for the attached cells that mitigates the effects of biocides and other toxic substances. The biofilm matrix is also sometimes referred to as "glycocalyx."

The architecture of biofilm consists of two main components: aqueous channels for nutrient transport and a region of densely packed cells having no prominent pores in it. The latter is often found in the base of the biofilm with a thickness of up to 5 to 50 μm. The colonies of bacteria, shaped like mushrooms or cones, can rise up to 100 to 200 μm. In a mature biofilm, the loosely organized glycocalyx matrix (75-95%) occupies a greater volume than that occupied by the planktonic bacterial cells (5-25%) (Prakash et al., 2003; Daniel et al., 2010).

1.4. Process of Biofilm formation

Most bacteria are capable of forming a biofilm where they spend a large fraction of their lifetime. Biofilm formation itself is a complex and multifactorial process in which microorganisms transform from planktonic to sessile mode of growth, and is regulated by different genetic and environmental factors. These factors include bacterial mobility as determined by two types of protein growths on their cell surface (flagella and fimbriae), cell membrane proteins (adhesins), extracellular polysaccharides, and signaling molecules (Monds and O'Toole, 2009). The process can be divided into at least five distinct stages as follows (Figure 1.2):

I. Initial attachment (adhesion or adherence) of planktonic cells

II. Irreversible attachment

III. Maturation I (microcolony formation)

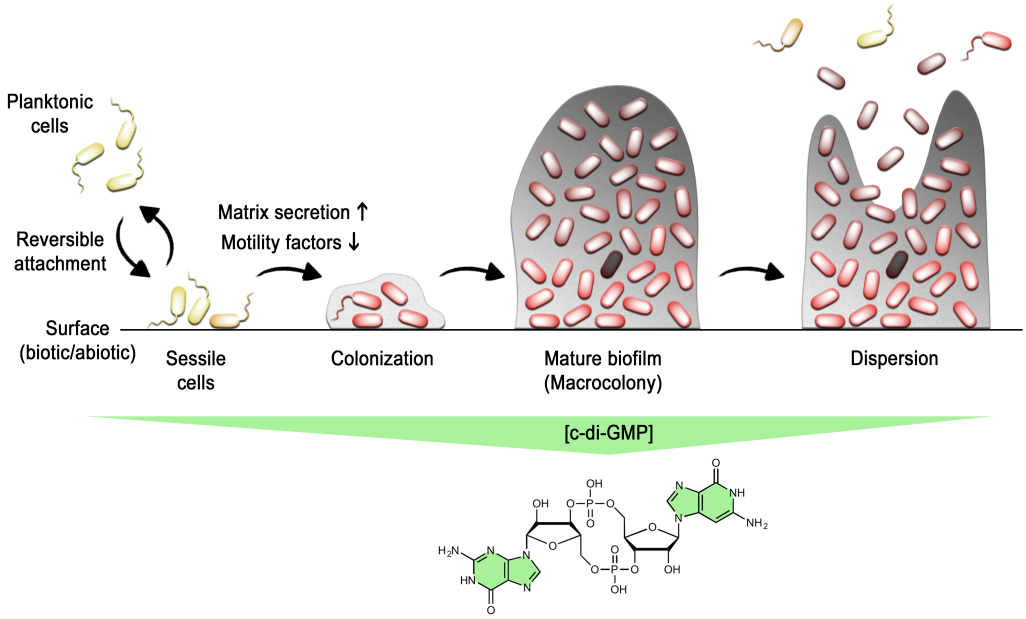

Figure 1.2. Overview of biofilm formation

Bacteria can reversibly attach to surfaces followed by loss of motility and synthesis of exopolysaccharides (EPS) and cellular adhesins. Mature biofilms are characterized by a complex architecture and collaborative behavior between functionally differentiated members. Finally, dispersal processes are governed by the secretion of glycolipid surfactants, proteases and nucleases, thereby leading to the release of highly motile planktonic cells, capable of colonizing new surfaces. A central regulator of this process is the bacterial second messenger c-di-GMP, whose chemical structure is shown below. High intracellular c-di-GMP levels (denoted by the thickness of the green bar) are typically associated with a biofilm lifestyle, while low levels characterize the free-swimming, planktonic or dispersion steps in the biofilm lifecycle.

Adapted from Chatterjee (2013)

IV. Maturation II (macrocolony formation), and

V. Dispersion

Stage I. Initial Attachment (Reversible)

Under favorable conditions, biofilm formation begins with the attachment of the planktonic microbial cells to surfaces that are rougher, more hydrophilic and coated by surface 'conditioning' films made up of organic molecules, proteins and complex polysaccharides. Conditioning films alter the characteristics of the substratum and allow microorganisms to adhere to the surface. The initial attachment is through weak, reversible electrostatic or van der Waals forces. During this step, flagella and type IV pili-mediated motilities are critical for initial interactions between cells and surface (O'Toole and Kolter, 1998; Monds and O'Toole, 2009). If the conditions are not favorable for microbial attachment, cells can detach from the surface.

Stage II. Irreversible Attachment

Once the initial contact is made, specific cell membrane proteins, called 'adhesins', maintain a stable connection between the microorganisms and the surface. Studies on *Escherichia coli* (Pratt and Kolter, 1998) and *Vibrio cholerae* (Watnick and Kolter, 1999) have shown that there is no biofilm formation if the adhesin activity is inhibited. Adhesin proteins differ in different bacterial species. The initial colonies facilitate the arrival of other planktonic cells by providing more diverse adhesion sites. The irreversibly attached biofilm can withstand stronger chemical and physical shear forces.

Stage III. Maturation I (Microcolony Formation)

Once the microorganisms are able to adhere to the biotic or abiotic surfaces irreversibly, the association becomes stable for microcolony formation. The initial colonies facilitate the arrival of other planktonic cells by providing more diverse adhesion sites. Once the microcolony formation begins, the biofilm grows through a combination of cell division and recruitment. It is during this step that cells are able to communicate with each other using signaling molecules ('quorum sensing', described below) that enable the microorganisms to organize into a community so that the biofilm functions as a multicellular organism.

The initial microcolony formation within a biofilm has been extensively studied in *Vibrio cholerae* O1 E1 Tor organism (Yildiz and Visick, 2009; Giglio et al., 2013; Teschler et al., 2015; Jones et al., 2015). The transition from a planktonic to a sessile lifestyle is regulated by c-di-GMP, which promotes the biosynthesis of the MshA (mannose-sensitive hemagglutinin) pili essential for attachment of the organism to surfaces. Once the initial attachment occurs, the MshA pilin assembly is dissociated into its constituent protein subunits by the action of MshE ATPase that results in altered motility and thus prepares the organism to switch from the motile to sessile phenotype (Jones et al., 2015). This is accompanied by a surge in EPS and the biofilm matrix proteins RbmA, RbmC and Bap1 synthesis to create the biofilm matrix within which the initial microcolony formation takes place.

Once the initial attachment takes place, the synthesis of autoinducers involved in the QS process organize the group behavior of the organism within the biofilm (Bassler and Losick, 2006; Eickhoff and Bassler, 2018).

Stage IV. Maturation II (Macrocolony Formation)

Once the microcolonies are formed, the transcription of specific genes that are required for the EPS synthesis takes place. Sometimes, the initial attachment itself can initiate the synthesis of the EPS matrix in which the sessile bacteria are embedded. The EPS matrix holds the biofilm together. Microorganisms that are not able to attach to a surface by themselves can often anchor themselves to the matrix or on to the earlier colonies, thereby creating the heterogeneity of various species that is often found in natural biofilms (Paraje, 2011). Aqueous channels are created within the biofilm for the circulation of nutrients and oxygen and for the removal of waste products from the communities of cells. During this stage, the biofilms may only change in size and shape. In a thick biofilm (>100 layers), bacteria are arranged according to their metabolism and oxygen tolerance. Anaerobic bacteria prefer to live in deeper layers of biofilm to avoid exposure to oxygen (Rabin et al., 2015). According to Mittelman (1996), the development of a mature biofilm may take from several hours to several weeks, depending on the system.

Stage V. Dispersion

Dispersion is a key survival strategy of a biofilm life cycle. At some point, the biofilm reaches a critical mass and a dynamic equilibrium is reached. Lack of nutrients, intense competition, outgrown populations, and changes in microenvironment within the biofilm (*e.g.,* pO_2) can disturb the equilibrium. As it ages, the biofilm cells have evolved mechanisms to escape the sessile mode of growth as a means of self-preservation and to colonize new spaces (Davies, 2011).

At least five different categories of detachment and dispersal have been identified (Petrova and Sauer, 2016): erosion, sloughing, human intervention, grazing, and abrasion. The first two refer to spontaneous detachment of cells from the biofilm. While erosion is due to continual detachment of small portions of biofilms or single cells closest to the bulk water interface, sloughing is the rapid loss of huge chunks of biofilm. Microbial cells can also be released due to abrasion when particles from the surrounding bulk liquid colloid with biofilms. The feeding activity of eukaryotic organisms can also remove biofilm cells by grazing.

A change from a sessile to a motile phenotype that allows the bacterial cells to leave a biofilm characterizes another mode of dispersion. During detachment process, the organisms preferentially express genes (e.g., transcription of pili and ribosomal proteins) that control motility and are typically seen in planktonic cells (Sauer et al., 2002). It also involves quorum sensing of certain signals or cues and their transduction through regulatory networks to enable physiological changes that weaken the biofilm EPS matrix and facilitate cellular release from biofilm communities (Petrova and Sauer, 2016). This type of dispersion occurs upon sensing of self-synthesized signaling molecules, as compared to environmentally induced dispersion. The latter is triggered by factors and changes in the external environment of the biofilm matrix. The organisms synthesize EPS matrix-degrading and adhesin dissolving enzymes (*e.g.,* alginate lyase, glycosyl hydrolase, or β-*N*-acetylglucosaminidase) or chemicals [*e.g., cis*-2-decenoic acid (cis-DA), nitric oxide, *cis*-11-methyl-2-dodecenoic acid (DSF)] that facilitate the detachment and release of cells from the surface (Hall-Stoodley et al., 2004; Petrova and Sauer, 2016). Although

the dispersed cells have the ability to retain certain properties of biofilms, they return quickly to their normal planktonic phenotype.

1.5. Cell-to-Cell Signaling (Quorum Sensing)

The development of biofilms on surfaces is mediated by density-dependent chemical signals released by bacterial cells densely packed within an EPS matrix. These conditions facilitate or may even represent the results of chemical communication between microbial cells. Quorum sensing (QS) thus is a cell-to-cell communication process or mechanism by which bacteria within a biofilm (and outside) community monitor cell density and regulate collective behaviors. Bacterial populations coordinate their gene expression by producing and responding to a variety of intra- and intercellular chemical signals termed 'autoinducers' (Camilli and Bassler, 2006). Autoinducers effect physiological changes in activities of cells when they reach a threshold concentration. In the QS process, microbial cells act as coordinator units rather than opportunistic individuals. QS also plays an important role in the dispersal of cells from matured biofilms. Examples of chemical signaling molecules include acyl-homoserine lactones (AHLs) in gram-negative bacteria, small peptides in gram-positive organisms, surfactin in *B. subtilis*, c-di-GMP in *Pseudomonas*, *Acetobacter*, and sRNAs in *E. coli* (Rabin et al., 2015; Lopez et al., 2010). Of these chemical signals, c-di-GMP is now proven to be an important regulator of several pathways that are coordinated or affected by QS (Valentini and Filloux, 2016; Boyd and O'Toole, 2012)

1.6. Regulation of Biofilm Formation

Several factors control the formation of biofilms in the nature. Some of these

are briefly described below.

Surface

The attachment of biofilms to both biotic and abiotic surface is a complex process. Because of less shear forces and increased surface area, biofilms are easily formed on rough surfaces (Characklis and Marshall, 1990; Prakash et al., 2003). Similarly, bacteria attach more readily to hydrophobic nonpolar surfaces (e.g., plastics) than to hydrophilic materials such as glass or metals.

Nutrients

The ready and abundant availability of nutrients increases the likelihood of biofilm formation, although nutrient concentrations too low to quantitate are also sufficient for biofilm growth.

Environmental Factors

The properties of the aqueous medium, such as pH, nutrient levels, iron, oxygen, ionic strength and temperature also influence the rate of biofilm formation.

Gene regulation

Once the initial interaction with the surface occurs, biofilm formation in microbial cells appears to be influenced by both up- and down-regulation of a number of genes. Numerous studies (reviewed by Goodman and Marshall, 1995) have shown that bacterial cells growing on solid surfaces within biofilms are in a physiological state different from that of planktonic cells, and show differential gene expression. In many bacterial species, regulation of metabolic functions, especially those related to virulence, involves cell-to-cell signaling molecules. Such mechanisms controlled by specific gene expression may play an important role in the establishment of the

biofilm-specific physiological state.

Prignet-Combaret et al. (1999) reported that 38% of the *E. coli* genes are differentially expressed in the biofilm, and directly control the response of the organism to microenvironmental conditions of osmolarity and oxygen concentration. Of these, 22% of the genes were up-regulated and 16% down- regulated during biofilm formation. The up-regulated genes include those involved in the formation and synthesis of EPS and adhesins as well as the ones involved in conferring resistance to antibiotics and biocides to prepare cells for a life in the biofilm matrix. Some examples include *algC* gene required for the synthesis of alginate (Davies and Geesey, 1995), porin *ompC* gene and the *proU* operon that encode a high-affinity glycine betaine transport system (Gowrishankar, 1985), genes encoding enzymes involved in glycolysis or fermentation in *Staphylococcus aureus* (Becker et al., 2001), and the *wcaB* gene involved in the synthesis of the capsular EPS colonic acid (Sledjeski and Gottesman, 1996). In contrast, motility-related genes expressing flagellum synthesis (*fliC* gene) or controlling the twitching motility of type IV pili are down regulated (O'Toole and Kolter, 1998; Prignet-Combaret et al., 1999). Reduced expression of motility-related genes allows the organisms to make a smooth transition from a planktonic to sessile life style.

1.7. Clinical Relevance

Biofilms formed by pathogenic microorganisms are a major health concern. They are difficult to eradicate by conventional antibiotic therapy and thus contribute to many chronic infections. Further, biofilm infections are often slow to produce overt clinically relevant symptoms. According to National Institutes of Health (NIH), about

65% of all microbial infections, and 80% of all chronic infections are associated with biofilms (Davies, 2003). Interest in biofilm formation by a group of clinically relevant bacteria that cause high mortality has been intensified. This group, known as ESKAPE, includes *Enterococcus faecalis*, *Staphylococcus aureus*, *Klebsiella pneumoniae*, *Actinetobacter baumannii*, *Pseudomonas aeruginosa*, and *Enterobacter* spp. (Rabin et al., 2015). Biofilm-forming microbial pathogens involved in several human diseases as well as in the contamination of various medical devices are summarized in Tables 1.1 and 1.2.

Some general features of biofilm infections in humans as compared to acute planktonic infections are summarized below (Abdel-Aziz and Aeron, 2014, Paraje, 2011).

1. Aggregates of bacteria embedded in a self-produced polymer matrix
2. Resistant to both innate and adaptive immune responses
3. Tolerant to clinically dosing of antibiotics despite susceptibility of planktonic cells, and
4. Chronic infections

Bacterial biofilms are less accessible to antibiotics and the human immune system, and thus pose a big threat to public health because of their involvement in several infectious diseases. Microorganisms inside a biofilm can also be protected against adverse conditions such as desiccation, osmotic shock, UV radiation, or exposure to toxic compounds or predators. The heterogeneous nature of biofilms may also give rise to multiple mechanisms of antimicrobial resistance (Paraje, 2011). Several factors contribute to the ability of biofilms to tolerate high concentrations of

Table 1.1. Clinically relevant biofilm-forming microbial pathogens

Biofilm-forming bacteria	Human diseases
Pseudomonas aeruginosa	Pulmonary and urinary tracts infections, cystic fibrosis, burn injury infections, blood infections
Yersinia pestis	Plague of Justinian, black death,
Klebsiella pneumoniae	Pneumonia, urinary and lower biliary tract wound infections
Legionella pneumophila	Legionnaires' disease
Vibrio vulnificus	Cellulitis, septicemia
Streptococcus spp.	Dental caries, endocarditis, childhood cystic fibrosis
Actinomyces oris	Dental caries
Staph. epidermidis *Staph. aureus*	Prosthetic joint infection, medical device-related infections
Corynebacterium spp. *Enterococcus* spp.	Endocarditis
Haemophilus influenza	Early childhood cystic fibrosis, otitis media
Enterobacter cloacae	lower respiratory tract infection, bacteraemia, urinary tract infections,
Escherichia coli,	Biliary tract infection, urinary catheter cystitis
Proteus mirabilis	Urinary tract infections

Compiled from Hall-Stoodley et al. (2004) and Rabin et al. (2015)

Table 1.2. Microorganisms commonly associated with biofilms on indwelling medical devices

Microorganism	Medical devices
Candida albicans	Artificial voice prosthesis Central venous catheter Intrauterine device (IUD)
Coagulase-negative Staphylococci	Artificial hip and voice prosthesis Central venous catheter Intrauterine device (IUD) Prosthetic heart valve Urinary catheter
Enterococcus spp.	Artificial hip prosthesis Central venous catheter Intrauterine device (IUD) Prosthetic heart valve Urinary catheter
Klebsiella pneumoniae	Central venous catheter Urinary catheter
Pseudomonas aeruginosa	Artificial hip prosthesis Central venous catheter Urinary catheter
Staphylococcus aureus	Artificial hip prosthesis Central venous catheter Intrauterine device (IUD) Prosthetic heart valve

From Donlan (2002)

antibiotics. Some mechanisms are listed below.

1. The EPS of biofilms may act as a diffusion barrier for the antimicrobial agents from surroundings into the biofilm.
2. Microorganisms within a biofilm have slow growth rates. Antibiotics, in contrast, are more effective in killing cells when they are growing actively.
3. Altered microenvironments within the biofilm (e.g., pH, oxygen content, gradients of physiological activity) also limit the efficacy of biocides.
4. The presence of persister cells, i.e., dormant variants of regular cells that are highly tolerant to antibiotics, which remain in a transient, dormant, and non-dividing state. These small subpopulations of bacteria within the biofilms can survive extreme antibiotic treatment. The changes in persister cells are often attributed to phenotypic variations rather than due to any stable genetic changes (Lewis, 2005). It is commonly believed that the presence of such persister cells within a community often makes complete eradication of biofilms quite difficult. In fact, the great diversity of metabolic stages coexisting within a biofilm ensures the survival of certain number of cells in case of any metabolic threat to the biofilm.
5. Due to the altered physiology within a biofilm, microorganisms may produce antagonist of antibiotics and develop novel degradation mechanisms (e.g., antibiotic-degrading enzymes, efflux pumps, membrane alterations) to render them ineffective (Paraje, 2011)

6. Altered gene expression by microorganisms within a biofilm community due to various stresses may also lower their susceptibility to antibiotics (Brown and Barker, 1999).

1.8. Beneficial Applications of Biofilms

Although most attention thus far has been focused on role of biofilms of pathogenic microorganisms in human health, biofilms do serve several beneficial functions. In the near future, it will be possible to engineer beneficial structured microbial communities that can be harnessed for constructive purposes. Some potential beneficial applications of structured biofilm-forming microbial communities include the following areas (Costerton, 2007; Kanematsu and Barry, 2015).

1. Bioremediation that does not require aggressive chemical remediation strategy to remove, detoxify, or immobilize numerous priority pollutants, e.g., polychlorinated biphyenls (PCBs), polyaromatic hydrocarbons (PAHs), oil spillage, and heavy metals
2. Developing microbial fuel cells (MFCs) that exploit microbial catabolic activities to generate electricity from complex organic wastes and renewable biomass, a great advantage over chemical fuel cells that utilize only purified reactive fuels (e.g., hydrogen)
3. Maintaining and improving the ecological health of freshwater rivers and streams by the decomposition of polysaccharides, peptides and organic phosphorus compounds
4. Wastewater and sewage treatment plants

5. In symbiotic relationship with important food crops for greater nutrient availability in marginal soils and for pathogen elimination
6. As green biosurfactants for use in pharmaceutical, cosmetics and food and agriculture industries
7. As a protein and enzyme delivery systems targeting abiotic surfaces, and
8. In developing strategies for building communities (novel probiotics) that are beneficial to human health.

1.9. Prevention and Control of Biofilms

Eradication of biofilms using conventional biocides and antimicrobials has proven quite difficult thus far. The heterogeneity of microbial populations within a biofilm community creates additional problems in designing novel antimicrobial agents and biocides. Although early intervention to eradicate biofilm infection using sufficiently high concentration of antibiotics is useful, any delay in implementing therapy often leads to treatment failure (Prakash et al., 2003). Thus, any treatment must be aimed at preventing biofilm formation rather than dispersal of the formed biofilm.

Commercially, several methods have been used with varying degrees of success to control and eliminate biofilm formation. Among the chemical methods, especially for indwelling medical devices and implants, antibiotics, biocides and ion coatings are routinely used to prevent biofilm formation. However, such treatment is often effective only for a short time period. The use of polysaccharide-hydrolyzing enzymes and oxidoreductases that degrade the EPS and release biofilm components and planktonic cells, which are then easily cleared by the immune system and drug

therapy, has also been tried (Xavier et al., 2005). The application of low intensity electrical current in combination with electromagnetic fields and ultrasound was also proven fairly effective both in vitro and in vivo in eradicating biofilms (Caubet et al., 2004; Rediske et al., 2000).

Biological control using bacteriophages, especially during the early stages of biofilm development was also tried to selectively eliminate specific species of bacteria from mixed-community biofilms (Huges et al., 1998). Similarly, a phage cocktail (combination of multiple phages) was also used for efficient and complete eradication of bacterial biofilms (Jamal et al., 2015).

Recently, a lot of attention has been given to understand quorum sensing and the signaling molecules that control the adhesion processes in biofilm formation. Since chemical signaling often controls the behavior of biofilms, one can manipulate both biofilm formation and detachment using these signals and their analogs. Understanding the underlying molecular mechanisms and both intra- and extracellular signals that cause differential gene expression will provide better diagnostic and treatment of chronic infections resulting from bacterial biofilms (Burmolle et al., 2014). Developing novel drug molecules that interfere with the cell-to-cell communication systems involved in biofilm formation and the manipulation of intrinsic and extrinsic resistance pathways thus appears to be a promising research area for the treatment of biofilm infections (Tolker-Nielsen, 2014; Kirmusaoglu, 2016).

CHAPTER 2

PSEUDOMONAS BIOFILM MODEL

Pseudomonas is a gram-negative, rod-shaped bacterium, capable of both aerobic and anaerobic growth and belongs to the bacterial family Pseudomonadaceae in the class of gammaproteobacteria. The family includes only members of the genus *Pseudomonas*, which are further subdivided into eight groups. *P. aeruginosa* is the type species of its group. Almost all strains of the genus are motile by means of a single polar flagellum. Commonly found in various types of moist environments, the organism easily adapts to several other conditions. It has the ability to survive on minimal nutritional requirements and to tolerate a variety of physical conditions that allow the organism to persist in both community and hospital settings (Lister et al., 2009).

P. aeruginosa is an opportunistic pathogen that easily exploits weaknesses in the host defenses to initiate an infection. It was amongst the first biofilm-forming human pathogens clinically isolated from the sputum of cystic fibrosis patients (Hoiby et al., 1977). The organism now accounts for over 10% of all hospital-acquired infections, is the fifth most frequently isolated nosocomial pathogen, and the second most frequently recovered pathogen from intensive care unit (ICU) patients (NNIS, 1998; Lister et al., 2009). Some of the most common human infections associated with this pathogen include septicemia, pneumonia, urinary and respiratory tract, ocular, ear and surgical site infections. Because of its ability to form biofilms on both biotic and abiotic surfaces, it is fairly tolerant to various antibacterial drugs and disinfectants and thus presents a serious therapeutic challenge. It is therefore critical

to look for novel strategies to treat infections caused by this pathogen. One potential strategy is to study the intra-cellular signaling mechanisms involved in biofilm formation and identify novel targets for drug discovery in these pathways. For our laboratory studies, *P. fluorescens*, being less virulent, was used to study bacterial biofilm formation. Also, its versatility and adaptation capabilities are linked with a broad range of complex regulatory networks, including a large set of genes involved in c-di-GMP biosynthesis, degradation, and transmission (Valentini and Filloux, 2016).

2.1. What Triggers Biofilm Formation?

Microorganisms have developed several mechanistic strategies to sense and respond to extracellular environments. This ability to sense, respond to, and adapt to their challenging environment is vital to the transition from a planktonic, free-floating to a sessile lifestyle to form biofilms. It is now widely recognized that microorganisms regulate adhesion to surfaces in response to both internal and external cues, including nutritional status of the cell or the availability of nutrients in the surrounding environment (Newell et al., 2011). The role of bacterial receptor proteins (often known as chemoreceptors) to convert extracellular signals into cellular responses and how bacteria integrate these signals to control various cellular processes has become of interest. Examples of chemical signaling molecules that control these processes include acyl-homoserine lactones (AHLs), small peptides, cyclic-di-GMP (c-di-GMP) and sRNAs (Rabin et al., 2015).

A common biofilm effector system found in over 1000+ bacterial genomes is the LapA/LapG/LapD system that is controlled by a bacterial second messenger, c-di-GMP. *P. aeruginosa* biofilms are estimated to contain on average 75-110 pmol of

c-di-GMP per mg of total cell extract, whereas planktonic cells contain less than 30 pmol/mg (Valentini and Filloux, 2016). C-di-GMP controls biofilm formation by regulating different outputs. These include surface attachment, flagellar motility, EPS production, adhesin localization, and transcriptional control of signaling pathways important for the initial surface attachment to convert to a sessile lifestyle (Giacalone et al., 2018; Dahlstrom et al., 2016). Some of the aspects of this signaling system in *P. fluorescens* are briefly reviewed below.

2.2. Cyclic Diguanylate (c-di-GMP) as a Second Messenger/Signaling Molecule

Cyclic-di-GMP was first discovered in 1987 as an allosteric regulator of cellulose synthesis in *Acetobacter xylinus,* now renamed as *Acetobacter xylinum* (Ross et al., 1987). Since then, it has emerged as a major bacterial second messenger implicated in several cellular functions, including but not limited to regulation of the cell cycle, differentiation, biofilm formation and dispersion, motility, virulence (Newell et al., 2009; Romling et al., 2013; Chatterjee et al., 2014). Enzymes involved in its synthesis and degradation have been identified in all major bacterial phyla, thus indicating its importance as a universal bacterial second messenger.

The dinucleotide is synthesized from two molecules of guanosine triphosphate (GTP) by GGDEF domain proteins with diguanylate cyclase (DGC) activity and is hydrolyzed by phosphodiesterases (PDEs) with either an EAL or a HD-GYP domain (Cooley et al., 2016). GGDEF domains catalyze the condensation of two molecules of GTP to generate c-di-GMP, while the EAL domains catalyze the hydrolysis of c-di-GMP to generate the dinucleotide 5’- phosphoguanylyl-(3’-5’)-guanosine (pGpG)

(Figure 2.1). Although a family of HD-GYP domain containing proteins is also able to hydrolyze c-di-GMP to produce GMP, an overwhelmingly large number of genes encoding the EAL domains in bacterial genomes indicate that the latter are the major phosphodiesterases responsible for maintaining cellular c-di-GMP concentrations (Ryan et al., 2006; Rao et al., 2008).

Although several proteins containing both GGDEF and EAL domains have been reported, many typically show either DGC or PDE activity and not both (Newell et al., 2011). These domains, either individually or in tandem, appear in combination with diverse regulatory domains commonly found in bacterial signaling proteins. These regulatory domains control the synthesis and degradation of c-di-GMP to external stimuli such as light, oxygen, or through post-translational modifications. Thus, many DGCs and PDEs respond directly to environmental signals and convert them into physiological responses with the help of c-di-GMP-binding receptors in many cellular signaling pathways (Sondermann et al., 2012).

An interesting observation is that despite the presence of multiple enzymes in bacteria that make or degrade c-di-GMP, these enzymes often confer distinct signaling outcomes in different cellular pathways (Cooley et al., 2016). For example, out of 30 predicted DGCs in *P. fluorescens* Pf0-1, mutations to only 4 caused significant reductions in biofilm formation (Newell et al., 2011), implying the most of the DGCs do not affect biofilm formation despite producing the same second messenger. One DGC preferentially affected LapA localization; a second controlled swimming motility, while a third one affected both LapA and motility. Thus there appears to be a signaling specificity between enzymes and receptors involved in c-di-GMP signaling.

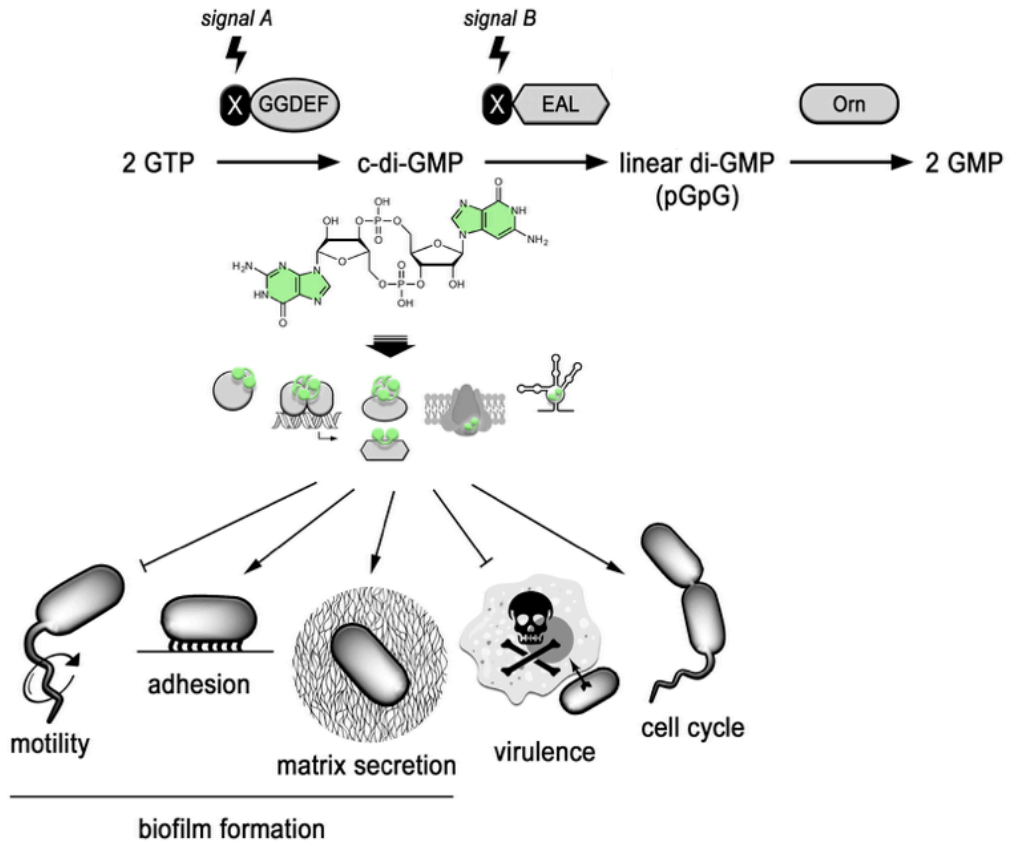

Figure 2.1. Cellular programs controlled by c-di-GMP

Two molecules of GTP are converted to c-di-GMP by diguanylate cyclases (DGCs) containing the GGDEF domain. C-di-GMP is degraded by phosphodiesterases (PDEs), which contain either EAL or HD-GYP domains. C-di-GMP regulates several cellular processes such as expression and activity of flagella, swimming and swarming (motility), adhesion to solid surfaces, synthesis of various adhesins and exopolysaccharides (adhesion, sessility and matrix formation), expression of acute virulence genes, and cell cycle progression.

Subsequently, Dahlstrom et al. (2015, 2016) identified a distinct DGC (GcbC) playing a specific role in contributing an activation signal, which relied on protein-protein interactions with LapD. Recently, Cooley et al. (2016) suggested that the flexibility of LapD in adopting many different conformations (e.g., apo- and c-di-GMP-bound states, LapD dimer and LapD dimer of dimers) allows for different interactions with other proteins for biofilm regulation. Mechanisms such as this would explain the apparent specificity of various DGCs and PDEs with effector proteins or receptors that depend upon c-di-GMP as a secondary messenger.

2.3. The Biofilm System in *Pseudomonas* spp. (LapA/LapG/LapD)

Biofilm formation in *Pseudomonas* spp. is mediated by c-di-GMP using the LapA/LapG/LapD effector system (Figure 2.2). LapA is a cell surface adhesion protein that is necessary for biofilm formation on a variety of surfaces and its localization is controlled by the activity of a periplasmic protease LapG, which is in turn controlled by the transmembrane receptor LapD. LapD transmits a cytosolic signal to the periplasm depending on whether or not it binds c-di-GMP. At high c-di-GMP levels in the cytosol, LapD binds the periplasmic protease LapG, and LapA remains associated with the cell surface and propagates biofilm formation. At low c-di-GMP levels, LapD undergoes a conformational change that reduces its affinity for LapG. LapG is free to move in the periplasm and cleaves off the periplasmic domain of LapA thus releasing LapA from the cell surface, weakening cell surface adhesion, and dispersing biofilms.

Much of the pioneering work in this field came from O'Toole and coworkers from their studies on P. *fluorescens* WCS365 and Pf0-1 strains. They identified

Figure 2.2. The LapA/LapG/LapD biofilm effector system

Biofilm effector system in *Pseudomonas fluorescens* consists of the inner membrane protein receptor LapD, the periplasmic protease LapG, and its target, the cell surface adhesion protein LapA (CdrA in *P. aeruginosa*). At high c-di-GMP levels, LapD sequesters LapG, allowing LapA to remain stably associated with the cell surface and promote biofilm formation. At low c-di-GMP levels, LapD undergoes a conformational change and adopts an auto-inhibited state (apo-LapD) that has low affinity for LapG. LapG is then free to cleave the N-terminus of LapA and release the adhesion from the cell surface, thus dispersing biofilms. GcbC is one of the DGCs involved in this signaling mechanism and contributes an activation signal that relies on protein-protein interactions with LapD.

Adopted from Cooley et al. (2016)

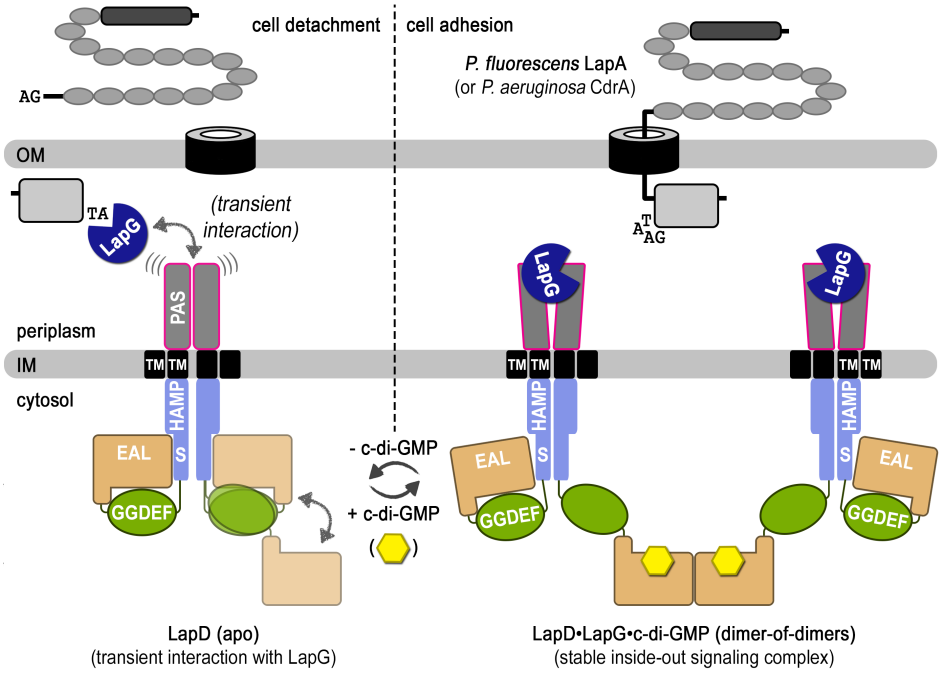
cell detachment
cell adhesion
AG
P. fluorescens LapA
(or P. aeruginosa CdrA)
OM
TA
LapG
(transient
interaction)
periplasm
IM
cytosol
PAS
TM
HAMP
S
EAL
GGDEF
- c-di-GMP
+ c-di-GMP
LapD (apo)
(transient interaction with LapG)
LapD•LapG•c-di-GMP (dimer-of-dimers)
(stable inside-out signaling complex)

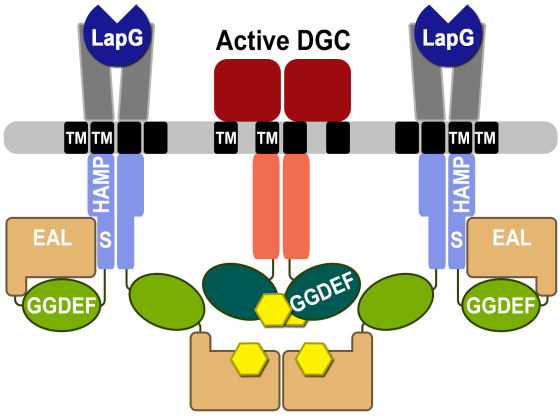
LapG
Active DGC
LapG
TM
HAMP
S
EAL
GGDEF

several transposon-generated mutations that rendered the bacterium unable to form a biofilm in the static assay system (O'Toole and Kolter, 1998a,b). When mutations were carried out in four specific adjacent genes, *lapA, lapE, lapB* and *lapC* (l*apAEBC* locus), the mutant strains could not make the transition from reversible attachment to the irreversible attachment stage of biofilm maturation (Hinsa et al., 2003). It was proposed that LapE, LapB and LapC form an ATP-binding cassette (ABC) transporter, while LapA was identified as a large adhesion protein essential for the irreversible attachment of the bacterial cells to a solid surface.

Using ORF (open reading frames) mapping techniques, O'Toole's group identified a sequence region (designated as *lapD*) adjacent to the l*apAEBC* locus that was essential for biofilm formation (Hinsa and O'Toole, 2006). Together, these genes constitute the Lap operon that controls cell adhesion and biofilm formation in gammaproteobacteria. They also observed that while it modulated the secretion of the LapA protein, LapD did not exert any influence on *lapA* transcription or LapA levels in the cytoplasm. This inner-membrane protein, however, did contain all the signature domains of proteins that catalyze the synthesis and degradation of c-di-GMP, although their active sites were degenerate.

LapD, which is exclusively localized to the inner membrane of *P. fluorescens*, is a homo-dimer of molecular weight of ~142kDa. Using ORF technique, Hinsa and O'Toole (2006) suggested that the *lapD* gene would encode a protein containing HAMP, GGDEF and EAL domains. The HAMP domain is commonly found in the cytoplasmic portion of a membrane-bound protein and is involved in transmitting signals from the periplasmic N-terminus to the cytoplasmic C-terminus of a protein

(Aravind and Ponting, 1999). Unlike other-c-di-GMP effectors identified, LapD is an inside-out signaling protein (Newell et al., 2009; Cooley et al., 2016). It is auto-inhibited at low cellular c-di-GMP levels and switches into a signaling-active state when c-di-GMP levels rise and bind to the cytoplasmic region of LapD. The ensuing conformational change transmits the signal for cytoplasmic c-di-GMP levels to the membrane-localized attachment machinery through a periplasmic output domain.

Proteins containing the GGDEF and EAL domains are known to posses DGC and PDE activities, respectively, and thereby control the intracellular levels of c-di-GMP. However, these two domains are degenerate and inactive in LapD and its EAL domain can only bind but not synthesize c-di-GMP. Mutations in the lapD gene prevented biofilm formation in *Pseudomonas fluorescens* by decreasing outer-membrane-associated LapA while increasing free, extracellular levels of LapA adhesin, and thus conformed the important role played by LapD in this pathway (Hinsa and O'Toole, 2006, Newell et al., 2009). Higher cell-surface-bound levels of LapA are required to initiate biofilm formation.

Recently, based on structure-function studies of a soluble LapD-LapG complex, Chatterjee et al. (2014) reported that the conformational changes that occurred in LapD on binding to c-di-GMP increased its affinity for binding to the protease LapG. Studies have shown that the binding of both c-di-GMP and LapG to LapD is essential for receptor activation. Recent work by Cooley et al. (2016) suggests that LapD forms a dimer-of-dimers 'receptor cradle' as its fully activated on-state and that this receptor cradle is required to interact with a subset of DGCs. GcbC is one such identified DGC that is involved in this signaling mechanism and

contributes an activation signal that relies on protein-protein interactions with LapD. Using a combination of cysteine crosslinking assays and size-exclusion chromatography coupled to multi-angle light scattering (SEC-MALS) techniques, Cooley et al. (2016) reported that LapD can adopt at least three global states as follows:

1. Dimeric apo-LapD
2. Dimeric LapD:c-di-GMP, and
3. LapD:c-di-GMP:LapG dimer-of-dimers complex

These studies further revealed that only a fraction of apo-LapD protomers adopt the auto-inhibited conformation at any given time, the binding of c-di-GMP to LapD leads to EAL domain dimerization that is accompanied by reorientation of its transmembrane helices, and the dimer-of-dimers formed upon LapG binding induces a distinct conformational change that activates the LapD receptor (Cooley et al., 2016).

2.4. Two-Component Signaling Pathway (TCS)

Microorganisms have developed several mechanistic strategies to sense and respond to extracellular movements. The ability to correctly sense different environmental stimuli via extracellular protein components and transduce these signals to intracellular domains is crucial for bacterial survival (Matamouros et al., 2015). Two-component signaling (TCS) pathways are ubiquitously present in prokaryotes as well as lower eukaryotes, where they control a wide array of cell functions (Capra and Laub, 2012; Stock et al., 2000). Unlike the majority of sensing and signal transduction in prokaryotes carried out by the so-called one-component systems (OCS), i.e., single proteins that combine properties of both a sensor and a regulator,

the TCS consists of two proteins: a sensor histidine kinase (component 1) and a response regulator (component 2) (Stock et al., 2000; Krell et al., 2010; Gushchin et al., 2017). Upon sensing environmental cues, the conserved histidine residue of sensor histidine kinase is autophosphorylated. The phosphoryl group from the histidine is subsequently transferred to a conserved aspartate residue in the response regulator. The resulting structural rearrangement elicits a change in target gene expression (Capra and Laub, 2012).

TCS systems are essential for cell growth, survival or pathogenicity, and thus offer a novel target to reduce virulence. These receptors generally function as homodimers and possess a periplasmic, membrane or intracellular sensor module, a transmembrane domain and often containing one or more of several intracellular signal transduction domains such as HAMP, PAS or GAF, and an intracellular auto-kinase module that phosphorylates the response regulator protein.

2.5. HAMP Domain as a Signal Transduction Element

The TCS pathways are commonly regulated by transmembrane chemoreceptors containing a conserved HAMP (**H**istidine kinases, **A**denylyl cyclases, **M**ethyl-accepting chemotaxis proteins and **P**hosphatases) domain that links the receptor input and output modules (Swain and Falke, 2007). The HAMP motif is thus an integral signal transduction element that interconverts different types of mechanical signals passing between modules. Many bacterial chemoreceptors exist as homodimers containing at least three functional modules. Each module plays a critical role in receptor-mediated signaling. The transmembrane-sensing module is composed of the sensing domain, which is typically present in the periplasm and contains the

ligand-binding site, the transmembrane portion of the chemoreceptor and an output domain that conveys this external environmental signal to the cell (Hazelbauer et al., 2008; Yeh et al., 1996; Khursigara et al., 2008). Since the HAMP domain in these receptors was proposed as the site of signal conversion between the transmembrane-sensing and kinase control modules, efforts were made to study its structure and its importance in signal transduction.

2.6. Structure of the HAMP Domain

Hulko et al. (2006) were the first to determine the structure of a HAMP domain of a putative archaeal transmembrane receptor, Af1503 by NMR spectroscopy. This protein is unusual in that it does not contain the cytoplasmic output domain typically coupled to the HAMP domain and thus lacks potential structural constraints from these cytoplasmic domains. This factor, and the origin of this protein from a thermophilic organism suggested that the HAMP domain would form a stable protein and thus make it easier to solve its structure. Hulko et al (2006) demonstrated that the HAMP domain folds into a parallel four-helix coiled-coil with each of the two α-helices composed of a heptad repeat (a-g) with hydrophobic residues in positions 'a' and 'd' pointing inwards to form a buried hydrophobic core. A flexible connector links the two helices of each monomeric unit.

HAMP domains from several chemoreceptors have been shown to be ~50 amino acids long and possess only a few conserved residues. They are alpha-helical regions that dimerize to form a parallel four-helix bundle with two α-helices, amphipathic sequence one and two (AS1 and AS2) from each monomeric unit (Hulko et al., 2006; Parkinson, 2010; Airola et al., 2013; Matamouros et al., 2015). The

secondary structural analysis of a broad range of various HAMP domains indicates that these domains generally consist of a helix-turn-helix fold (Aravind and Ponting, 1999).

2.7. Models for HAMP Domain Signaling Mechanisms

Several models have been proposed to describe the molecular motions of HAMP domains during signal transduction. These models are not necessarily mutually exclusive and include: 1) a swinging piston mechanism (Chervitz and Falke, 1996; Falke and Hazelbauer, 2001), 2) the gearbox model (Hulko et al., 2006; Ferris et al., 2012), and 3) a dynamic model of four-helix bundle stability (Zhou et. al 2009).

The piston displacement model replaced an early model proposing a scissors-type displacement of two subunits (Milburn et al., 1991) by providing proof that the subunit interface remains static during activation and inactivation (Chervitz et al., 1995; Hughson and Hazelbauer, 1996). Chervitz and Falke (1996) proposed the swinging-piston model for aspartate receptors. From a combination of x-ray crystallographic studies (Milburn et al., 1991), ^{19}F NMR (Danielson et al., 1994) and disulfide scanning experiments (Chervitz and Falke, 1995), they compared the apo and aspartate-bound structures and revealed that aspartate-induced movement is a 'swinging–piston' displacement of the second transmembrane helix where it moves perpendicular to the membrane. The signal is transmitted by the movement of a single transmembrane helix that is located in the subunit that provides most of the contacts to the bound aspartate. This was postulated to involve both a translational piston and a rotational swinging component, which then alters the structure of the cytoplasmic

signaling domain. This displacement can fully communicate the aspartate-induced signal across the bilayer.

Hulko et al. (2006) and Ferris et al. (2012) proposed the two-state gearbox model based on a series of NMR and x-ray crystallographic structures of the HAMP domain. The NMR-based structure of the HAMP domain of Af1503 revealed an unusual *x-da* packing arrangement of helices in the bundle rather than the conventional *a-d* packing found in canonical coiled coils. Hulko et al. (2006) proposed that the HAMP domain conveys its signal by switching between these two nearly iso-energetic states by a 26° counter-rotation of each of the four helices, analogous to meshed gears in a transmission.

Later on, Zhou et al. (2009) suggested that HAMP domains are dynamic and transmit signals by adopting a variety of conformational states of differing stabilities rather than a few discrete conformational states. Based on the studies of a serine chemoreceptor in *E. coli*, Tsr, they proposed that HAMP domains may operate over a portion of their dynamic range, the most stable of which could be the 4-helix *x-da* bundle and the least stable would be a fully denatured bundle.

2.8. The LapD HAMP domain

Although there is a lack of sequence similarity, we used the HAMP domain structure determined by Hulko et al (2006) to generate homology models with that of LapD's HAMP domain. Such an approach should be feasible since studies have shown that while the HAMP domains among different chemoreceptor proteins tend to

be divergent, a conservation of helical amphipathicity rather than specific amino acid residues is important for their function (Williams and Stewart, 1999).

The HAMP domain is also found in DGCs (GGDEF), DGCs/PDEs (GGDEF/EAL), metal-dependent phosphohydrolases (HDc) and Ser/Thr/Tyr protein kinases (STYKc) (Dunin-Horkawicz and Lupas, 2010). It links the transmembrane domains with the enzymatic or functional cytoplasmic domains, thereby facilitating signal transduction across the membrane to modulate the activities of the cytoplasmic domains (Kumita et al., 2003; Ward et al., 2006). Deletion of HAMP domains in transmembrane receptors disrupts the link between input and output units, generating receptors that are incapable of switching activity states upon stimulation (Hazelbauer et al., 2008).

Recently, Chatterjee et al. (2014) reported the molecular mechanism by which LapD and LapG interact in *P. fluorescens* and the importance of HAMP domain in LapD for modulating these interactions. Upon binding to c-di-GMP, LapD adopts a conformation that allows it to bind to LapG with greater affinity. It was speculated that the shape compatibility is more important than any chemical interactions between the amino acid side chains of the protein that enhances the affinity of LapD for LapG protease. Chatterjee et al. (2014) also found that biofilm formation can be easily manipulated by disrupting the LapD-LapG interactions to varying degrees.

The HAMP domain of LapD appears to play an important role in LapD-LapG interactions. The periplasmic domain of LapD that binds LapG is flanked by two putative transmembrane helices, one of which connects the intracellular HAMP

domain and in turn the GGDEF-EAL domain module in the cytoplasm (Navarro et al., 2011; Newell et al., 2011, Boyd and O'Toole, 2012). The overall process by which conformational changes are transmitted through the protein via HAMP domains and how they result in a change of affinity for LapG is still poorly understood. Much still remains to be elucidated at the molecular level, especially the signaling mechanisms and the associated conformational changes in these proteins that are crucial for cell adhesion and thus the formation of a stable biofilm.

This study was undertaken to fill some of these gaps in our knowledge, focusing on the molecular mechanism of the transmembrane c-di-GMP receptor LapD, the main signaling switch in this pathway. It is proposed that LapD forms a dimer-of-dimers receptor cradle to transmit the cytosolic c-di-GMP signal to the periplasm. The coordinated conformational changes of LapD on either side of the membrane and how these are regulated to attain a signaling on-state of the receptor are still not fully understood. In this study, we have used cysteine crosslinking experiments to further characterize the HAMP domain and catalog changes in LapD as a function of activation state. An understanding of this process would shed more light on how bacterial cell signaling systems work and may offer novel drug targets to control biofilm formation. It also sets the stage for future studies to map the conformational changes associated with protein-protein interactions in c-di-GMP signaling networks.

CHAPTER 3

MATERIALS AND METHODS

Unless mentioned otherwise, all chemicals used were of the highest purity available commercially. The following abbreviations were used. IPTG: isopropyl-1-thio-β-D-galactopyranoside; LMNG: Lauryl maltose neopentyl glycol; TCEP: tris(2-carboxyethyl)phosphine; CHAPS: (3-((3-cholamidopropyl) dimethylammonio)-1-propanesulfonate); NTA: nitrilotriacetic acid; EPR: Electron paramagnetic resonance; SOC: Super optimal broth with catabolite repression

3.1. Site-directed Mutagenesis

LapD-msfGFP single-cysteine mutants spanning the HAMP domain and S-helix (residues 171-237) and selected periplasmic domain mutants were generated using the Quikchange-II Site-Directed Mutagenesis kit (Agilent Technologies, Santa Clara, CA). The procedure uses a supercoiled double-stranded DNA (dsDNA) vector with the insert of interest and two synthetic oligonucleotide primers, both containing the desired mutation. The primers, which were each complementary to opposite strands of the vector were extended during PCR by PfuUltra HF DNA polymerase without displacing the primers. This generated a mutated plasmid containing staggered nicks. The product was then treated with DpnI endonuclease, which targets methylated and hemimethylated DNA and digests the parental DNA template.

The nicked vector DNA containing the desired mutation was then transformed into Stellar competent cells (Takara Bio USA, Mountain View, CA). Colonies were picked and cells were grown overnight at 37°C in Lysogeny broth (LB). DNA

extraction was done using the NucleoSpin DNA extraction Kit (Takara Bio USA, Mountain View, CA). The presence of the mutation was verified by DNA sequencing.

3.2. LapD-msfGFP Protein Expression and Membrane Isolation for Crosslinking

LapD fused C-terminally with monomeric superfolder GFP (msfGFP)-His_6 was expressed from a pET-28 based vector. LapD-msfGFP fusion proteins were overexpressed in *E. coli* BL21 T7 express cells (New England Biolabs, Ipswich, MA). Cells were transformed by incubating ~50 ng of plasmid DNA with 50 µl of cells on ice for 20 min, followed by heat shock at 42°C for 45 sec. Cells were recovered by incubating in a shaker-incubator in 250 µl of SOC media at 37°C for 1 hr. The entire cell suspension was plated on pre-warmed LB agar plates with selection antibiotic (50 µg/ml kanamycin) and incubated overnight at 37°C. The next day, colonies were picked and cell cultures grown at 37°C in Terrific Broth (TB) media supplemented with 50 µg/ml kanamycin. The temperature was reduced to 18°C at an OD_{600} of ~1 and protein expression was induced by adding 0.5 mM IPTG. Expression was allowed to proceed for 16 hr, after which cells were harvested by centrifugation at 4000g for 20 min and resuspended in lysis buffer (25 mM Tris pH 7.5, 150 mM NaCl, 5% glycerol). Cells were lysed by sonication and membranes were pelleted by ultracentrifugation at 100,000g for 20 min. The supernatant was discarded and the membranes were resuspended in lysis buffer, flash frozen in liquid nitrogen, and stored at -80°C until further use.

To prepare LapD-msfGFP for crosslinking experiments, membranes were solubilized in 25 mM Tris-HCl pH 7.5, 150 mM NaCl, 5% glycerol, 2 mM $MgCl_2$, 2

mM $CaCl_2$, 1% (w/v) LMNG, 0.1% (w/v) CHAPS for 90 min at 4°C. Insoluble material was pelleted by ultracentrifugation at 100,000g for 20 min. The supernatant containing the detergent-solubilized protein was collected and the concentration of solubilized LapD-msfGFP was determined by measuring the absorbance at 488 nm using an extinction coefficient of 83,000 $M^{-1}cm^{-1}$. LapD-msfGFP was used in crosslinking experiments immediately after solubilization.

3.3. LapG Expression and Purification

LapG lacking the signal peptide (residues 50-251) was expressed as an N-terminal His_6-tagged fusion protein from a pET21 expression vector. The protein was overexpressed in *E. coli* BL21 T7 express cells. Cell cultures were grown at 37°C in Terrific Broth (TB) media supplemented with 100 μg/ml ampicillin. The temperature was reduced to 18°C at an OD_{600} of ~1, and protein expression was then induced by adding 0.5 mM IPTG. Expression was allowed to proceed for 16 hr, after which cells were harvested by centrifugation at 4000g for 20 min. Cells were resuspended in Ni-NTA buffer A (25 mM Tris-HCl pH 8.5, 500 mM NaCl and 20 mM imidazole), flash frozen in liquid nitrogen, and stored at -80°C. After thawing cells and lysing by sonication, cell debris were removed by centrifugation. The lysates were incubated with Ni-NTA resin (Qiagen, Germantown, MD) and equilibrated with Ni-NTA buffer A. The resin was washed with 10 column volumes of Ni-NTA buffer A prior to eluting LapG with 3 column volumes of Ni-NTA buffer B (25 mM Tris-HCl pH 8.5, 500 mM NaCl and 350 mM imidazole). LapG was then buffer exchanged into desalting buffer (25 mM Tris-HCl pH 8.5, 500 mM NaCl) on a fast desalting column (GE Healthcare), concentrated and subjected to size-exclusion chromatography on a

Superdex 200 column (GE Healthcare) equilibrated with gel filtration buffer (25 mM Tris-HCl pH 8.5, 400 mM NaCl). Purified LapG was concentrated (>20 mg/ml) on Amicon filters with a 10 kDa molecular weight cut-off, flash frozen in liquid nitrogen and stored at -80°C.

3.4. Cysteine Crosslinking

Crosslinking experiments were performed using variants of LapD-msfGFP lacking all four native cysteines (Cysless construct: C12A/C158A/C304A/C397S) except for the S229C/A602C mutant, which retains the two native transmembrane cysteines (C12 and C158). The disulfide bond promoting copper phenanthroline [$Cu(Phen)_2$] catalyst was freshly prepared by mixing stocks of 200 mM 1,10-phenanthroline in ethanol and 200 mM $CuSO_4$ in appropriate ratios to yield 4 mM $Cu(Phen)_2$. For each mutant, the following five-crosslinking conditions were set up:

1. apo LapD with no catalyst added,
2. apo LapD with catalyst present,
3. LapD incubated with c-di-GMP before adding catalyst,
4. LapD incubated with LapG before adding catalyst, and
5. LapD incubated with both c-di-GMP and LapG before adding catalyst.

For the crosslinking reactions set up to reduce background crosslinking in the absence of catalyst, samples were first incubated with a 100-fold molar excess of TCEP for 30 min at room temperature before proceeding. For each reaction, 1 μM LapD was incubated with or without 5 μM LapG and/or 25 μM c-di-GMP for 15 min at room temperature. $Cu(Phen)_2$ catalyst was then added to 100 μM final concentration to initiate cysteine crosslinking and the samples were incubated for an

additional 15 min. The reaction was quenched by adding 10 mM EDTA and 20 mM N-ethylmaleimide and immediately analyzed by SDS-PAGE on an 8% (w/v) polyacrylamide gel. Gels were imaged by fluorescence on a Biorad ChemiDoc system. Experiments were done with n=1, except for the S229C/A602C mutant, for which multiple trials were conducted.

3.5. LapD Purification and MTSL Labeling for Electron Paramagnetic Resonance (EPR) Studies

Cysless LapD-His_6 with the desired single cysteine substitution was expressed from a pET-24 based vector. Similar transformation, cell culture and harvesting procedures were followed as for the LapD-msfGFP fusion protein described previously. Harvested cells were flash frozen in liquid nitrogen and stored at -80°C until further use.

Cells were thawed and 0.5 mg/ml lysozyme was added before lysing cells by sonication. Membranes were pelleted by ultracentrifugation at 100,000g for 1 hr at 4°C. The supernatant was discarded and membranes were resuspended in membrane buffer (25 mM Tris pH 7.5, 500 mM NaCl, 10% glycerol), flash frozen in liquid nitrogen and stored at -80°C. Membranes were thawed and solubilized in membrane buffer supplemented with 2% Triton X-100 (Sigma Aldrich) for 90 min at 4°C. Insoluble material was then pelleted by ultracentrifugation at 100,000g for 45 min. The supernatant containing detergent-solubilized protein was incubated with Ni-NTA resin equilibrated with membrane buffer and then washed with 20 column volumes of membrane buffer supplemented with 4 mM β-mercaptoethanol, 20 mM imidazole and 1% Triton X-100. The Triton X-100 detergent was exchanged for 0.01% (w/v)

LMNG in a step-wise manner followed by elution of LapD with elution buffer (25 mM Tris-HCl pH 7.5, 500 mM NaCl, 5% glycerol, 300 mM imidazole, 0.01% (w/v) LMNG).

For EPR experiments, to reduce any disulfide bonds already present within the protein before labeling with spin label, LapD was incubated with 50-fold molar excess of TCEP at 4°C for 45 min. LapD was then buffer-exchanged into low-salt desalt buffer (25 mM Tris-HCl pH 7.5, 150 mM NaCl, 5% glycerol, 0.01% (w/v) LMNG) on a fast desalting column (GE Healthcare) to remove the reducing agent. LapD was concentrated to ~50 μM before spin-labeling with S-(2,2,5,5-tetramethyl-2,5-dihydro-1H-pyrrol-3-yl)methyl methanethiosulfonothioate (MTSL; Toronto Research Chemicals). MTSL was dissolved in acetonitrile and added to protein solution at 30-fold molar excess concentration. The labeling was performed for 4 hr at room temperature and continued for additional 12 hr at 4°C. Unreacted spin label was removed by size exclusion chromatography into gel filtration buffer [25 mM Tris-HCl pH 7.5, 150 mM NaCl, 0.0025% (w/v) LMNG, 0.02% (w/v) CHAPS] on a Superdex 200 column (GE Healthcare). Purified, spin-labeled LapD was buffer exchanged into gel filtration buffer containing 30% glycerol in a step-wise manner using Amicon centrifuge concentrators and concentrated to 10-100 μM for EPR measurements.

Dr. Peter Borbat at the National Biomedical Research Center for AdvanCed ESR Technology (ACERT) analyzed the samples.

3.6. GcbC–LapD Co-expressions

For the co-expression of LapD and GcbC in *E. coli*, GcbC-His_6 was cloned into a vector having different origin of replication and antibiotic resistance than the

pET28a-LapD construct. GcbC-His_6 was amplified by standard PCR from a pET21-GcbC construct and cloned into multiple cloning site 1 (MCS1) of the vector pACYCDuet-1 (Novagen) via In-Fusion cloning (Takara Bio USA, Inc.), following the manufacturer's instructions.

LapD-msfGFP and GcbC fusion proteins were co-expressed in *E. coli* BL21 T7 express cells. Cell cultures were grown at 37°C in Terrific Broth (TB) media supplemented with 50 μg/ml kanamycin and 34 μg/ml chloramphenicol. Cells were induced with 0.5 mM IPTG and membranes containing LapD and GcbC were isolated and frozen for crosslinking studies as previously described.

3.7. ImageJ Densitometric Analysis

Gels imaged by fluorescence on a Biorad ChemiDoc system were exported as 600 dpi TIFF files for ImageJ (NIH)-based band quantification. Images used for ImageJ analysis were taken with exposure times of 1-2 sec such that the images obtained were of good quality without any bands showing signs of saturation. Regions of equal areas were marked off around each band of interest and the raw integrated density was measured. The background was subtracted from each of these values. For each lane, the percentage of LapD that was present in its crosslinked/disulfide-dimerized form was calculated. Results were summarized in a plot for easy visualization of the amount of protein crosslinked across the five different conditions.

For the A602C/S229C LapD mutant, statistical analysis was done using GraphPad Software (San Diego, CA). Scatter dot plots were plotted with the error bars representing the standard deviation.

3.8. HAMP Domain Homology Models Based on Solved Af1503 Structure

The LapD HAMP domain dimers were modeled based on the NMR and crystallographic structures of the HAMP domain of the protein Af1503 reported in Ferris et al. (2011). The program MODELLER (Fiser and Sali, 2003) was used to implement comparative protein structure modeling using the method of satisfaction of spatial restraints. Modeling was performed by Dr. Holger Sondermann.

CHAPTER 4

RESULTS AND DISCUSSION

4.1. Cysteine Crosslinking as a Method to Probe Conformational Changes in LapD

In this study, conformational changes in LapD's HAMP domain were mapped using site-directed cysteine and disulfide chemistry (Falke and Koshland, 1987). This method reveals a wide range of information about the structure and regulatory mechanics of a protein. It can be used to map out 2°, 3° and 4° structure, analyze conformational changes and covalently trap a protein in various active or inactive states. This approach can be especially useful to obtain structural information about proteins that are resistant to high-resolution techniques (Bass et al., 2007). The structure of full-length LapD has proven difficult to obtain by X-ray crystallography, and thus this is a useful method to both gain insight into conformational changes occurring on protein activation and also provide structural constraints that could stabilize LapD and make it more amenable to crystallographic and/or cryo-electron microscopy techniques.

Though crystal structures of distinct functional states of LapD's periplasmic and cytosolic domains have been solved (Chatterjee et al., 2014; Navarro et al., 2011), no such information is available for its HAMP domain and S-helix. The S helix is a conserved helical segment that is typically found between two signaling domains in a variety of signaling proteins (Ananthraman et al., 2006). In LapD, the S-helix is a continuation of the second HAMP domain helix and is believed to be involved in

transducing signals through the HAMP domain to the adjacent signaling modules (Navarro et. al, 2011).

Disulfide mapping and cysteine crosslinking is a useful method to both gain structural information and study conformational changes occurring in LapD during different modes of activation. Disulfide mapping measures disulfide bond formation rates and can be used to identify contacts between two residues in the 3° and 4° structures of a protein. This gives information about protein structure in different signaling states and helps define conformational changes that link different states (Bass et al., 2007). The disulfide mapping approach is based on the assumption that under identical oxidizing conditions, proximal cysteine pairs will collide and form disulfide bonds quicker than distal cysteine pairs. For a disulfide bond to form, the β-carbon–β-carbon distance must be ≤4.6 Å and the cysteine residues must collide with specific angular orientations (Swain and Falke, 2007).

In this study, we introduced single amino acid cysteine mutations spanning the entire HAMP domain and S-helix in the LapD-monomeric superfolder GFP (msfGFP) fusion protein lacking the four cysteines present in native LapD (cysteine-less or cysless construct: C12A/C158A/C304A/C397S). The advantage of using such a construct is that each engineered cysteine becomes a unique site for disulfide chemistry, thus making the analysis simpler and the information easier to interpret. Earlier studies from our laboratories using LapG binding assays (Chatterjee et al., 2014) and SEC-MALS analyses (Cooley et al., 2016) have also shown that the msfGFP fusion protein, and the cysless and TMcys (LapD retaining its two transmembrane cysteine residues, C12 and C158) variants of LapD retain their

function and that the cysteine mutations do not notably perturb the receptor conformation and function.

Introducing cysteine substitutions does not typically perturb protein structure as the cysteine side-chain is relatively small, sterically accommodating and the sulfhydryl group can switch between apolar, protonated and deprotonated states to adapt to different electrostatic environments. Several studies suggest that unless the cysteine residue is required for folding stability, cysteine substitutions are well tolerated even when located at buried positions (Careaga and Falke, 1992; Falke and Koshland, 1987; Falke et al., 1986). Thus, the cysteine mutations introduced in LapD mapping the HAMP domain should not noticeably affect its function.

Four distinct states of LapD were considered in these experiments: 1) apo, 2) in the presence of c-di-GMP, 3) in the presence of LapG, and 4) in the presence of both c-di-GMP and LapG. C-di-GMP and LapG alone are considered to be partial activators of LapD, and together they bring about a conformational change that leads to the formation of LapD dimers-of-dimers. As LapD exists as a homodimer as its smallest functional unit, a single amino acid substitution is represented once in each monomeric unit and the intra-dimer crosslinking of these residues was reported. Cysteine crosslinking experiments were performed on these four states of LapD by mildly oxidizing the protein in the presence of the catalyst copper phenanthroline [$Cu(Phen)_2$] as per the method described in Cooley et al. (2016). The presence of disulfide dimer formation was detected using in-gel fluorescence. Crosslinks introduce electrophoretic mobility shifts of the msfGFP-fusion protein and these can be easily visualized by the higher molecular weight band shift on SDS-PAGE gels.

4.2. Cysteine Crosslinking on the LapD-msfGFP TMcys A602C/S229C Mutant

The LapD-msfGFP TMcys A602C/S229C mutant was chosen based on the crystal structures of the cytoplasmic domain of apo- and c-di-GMP-bound LapD (Navarro et al., 2011). Residues S229 of the S-helix and A602 of the EAL domain of the same polypeptide chain are in close proximity and are thus suitable candidates for crosslinking studies. A602C allows us to probe EAL domain dimerization and together with S229C allows us to probe S helix-EAL domain contacts. This mutant is thus a suitable reporter of the activated and auto-inhibited states of LapD (Cooley et al., 2016) (Figure 4.1).

Cysteine crosslinking reactions on detergent solubilized membrane fractions were performed for the five different cases: 1) apo LapD without oxidant, 2) apo LapD with oxidant added, 3) LapD-c-di-GMP bound protein with oxidant added, 4) LapD-LapG bound protein with oxidant added, 5) LapD-c-di-GMP-LapG bound protein with oxidant added, and each individual condition is represented in a single lane of the gel(Figure 4.2). In the absence of any oxidizer, there is a low-level of disulfide dimer formation, formed by the intra-molecular A602C~S229C crosslink in the apo-protein. The extent of crosslink increases upon mild oxidation with $Cu(Phen)_2$, as evidenced by the increase in band intensity on SDS-PAGE gel. These bands represent the protein locked in the auto-inhibited state.

Upon incubating with one of the partial activators of the system, c-di-GMP (case 3 in the above list), prior to oxidation, LapD undergoes a conformational change creating a new population of crosslinked protein, which has slower electrophoretic

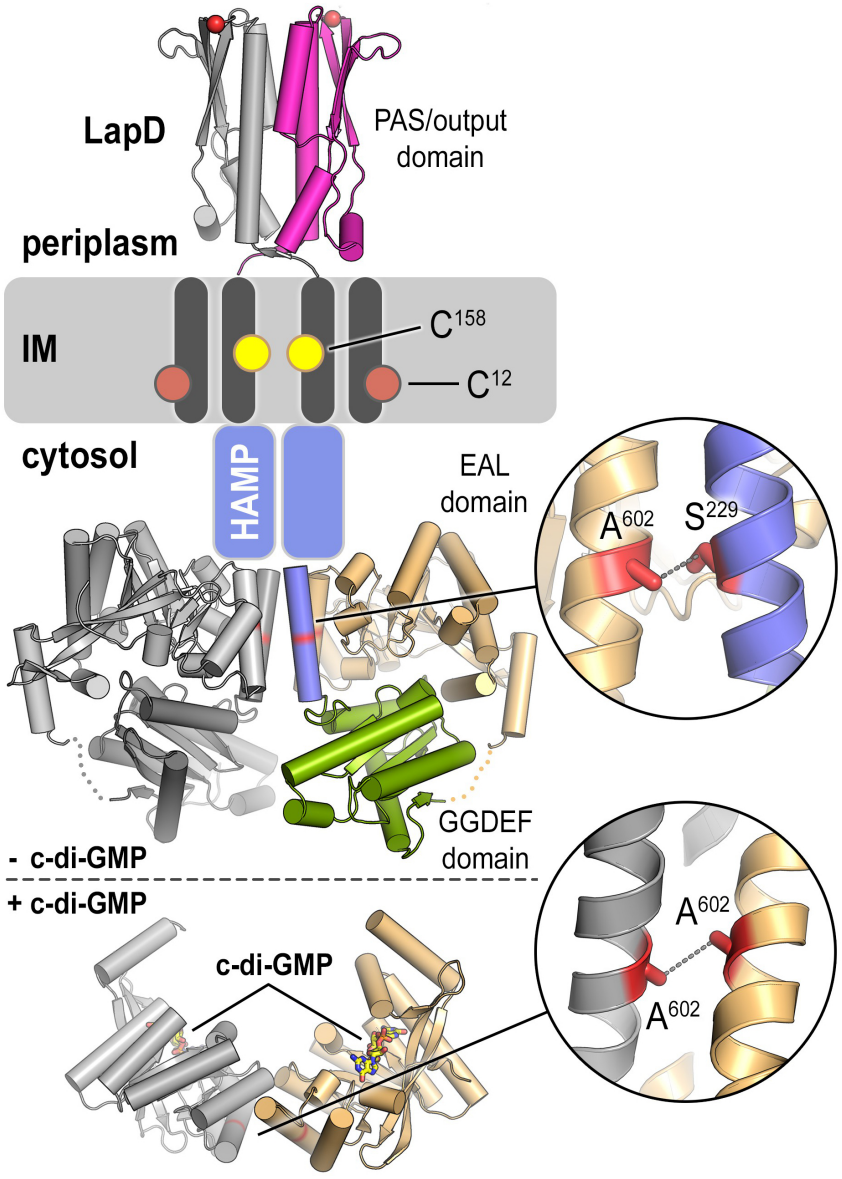

Figure 4.1. Composite model of LapD based on available crystal structures

The A602C~S229C intramolecular crosslink (auto-inhibited LapD) and A602~A602C intradimer crosslink (c-di-GMP bound LapD) are represented.

From Cooley et al. (2016)

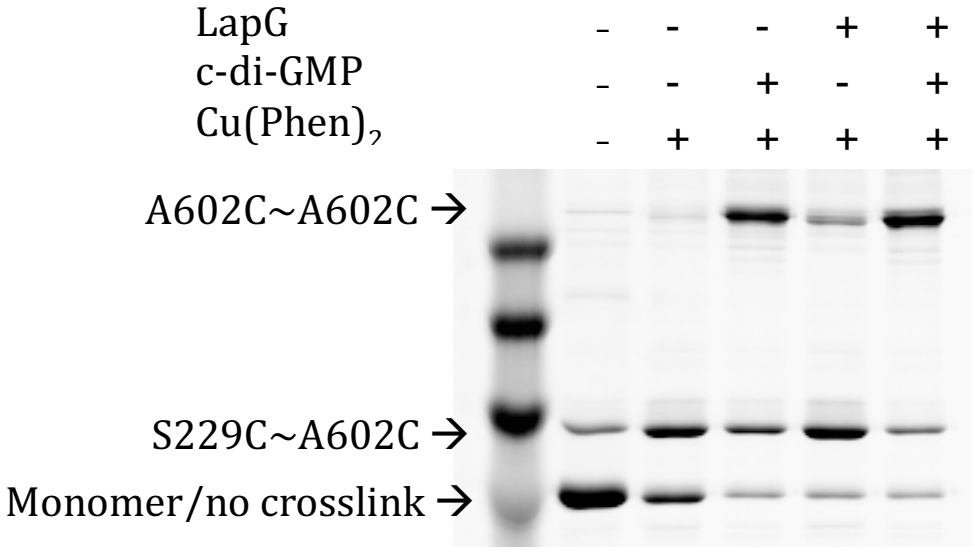

Figure 4.2. Cysteine crosslinking on the LapD TMcys (C304A/C397S) A602C/S229C mutant.

Detection of intramolecular and intradimer disulfide bonds using in-gel fluorescence. Samples used for this gel were TCEP-treated.

mobility. This represents the activated or c-di-GMP bound state of LapD. This crosslink was identified as the A602C~A602C crosslink from previous crosslinking experiments done with the LapD cysless-A602C mutant lacking the S229C mutation (Cooley et al., 2016). This close proximity of A602C residues indicates the formation of c-di-GMP-dependent EAL domain dimers (Navarro et al., 2011; Barends et al., 2009; Sundriyal et al., 2014). A small amount of protein locked in the auto-inhibited state remains, which accounts for the spontaneously oxidized protein already present prior to activation and facilitated oxidation.

For case 4, LapD was incubated with its other partial activator, LapG prior to oxidation. A smaller amount of activated LapD (as judged by the band intensity) was observed as compared to that in the presence of c-di-GMP. This confirms that LapG binding to LapD in the absence of c-di-GMP can also trigger this conformational change, albeit at a slower rate. This may be due to the fact that LapG-LapD binding is transient in the absence of c-di-GMP (Chatterjee et al., 2014) and/or by the fact that this signal needs to be transmitted across the inner membrane.

When both activators, c-di-GMP and LapG, were allowed to bind to LapD prior to oxidation, a small increase in crosslinking via corresponding A602C residues was observed when compared to that in the absence of LapG. This was more easily seen through the ImageJ-based quantification of multiple replicates of this experiment (Figure 4.3). The tight distribution of the replicates indicates how robust the assay is.

4.3. HAMP Domain and S-helix Mapping via Cysteine Crosslinking

LapD single-residue cysteine mutants spanning the HAMP domain (residues 171-222) and the S-helix (residues 223-237) were generated and used for crosslinking

Figure 4.3. ImageJ quantification of band intensities for TCEP-treated gels

Each plot represents a single lane in the gel. The percentage of protein in each lane corresponding to each crosslinked or non-crosslinked state was reported (n = 15). Error bars represent standard deviation.

A: Apo-LapD without oxidant
B: Apo-LapD with oxidant
C: c-di-GMP-bound LapD with oxidant
D: LapG-bound LapD with oxidant
E: c-di-GMP-LapG-bound LapD with oxidant

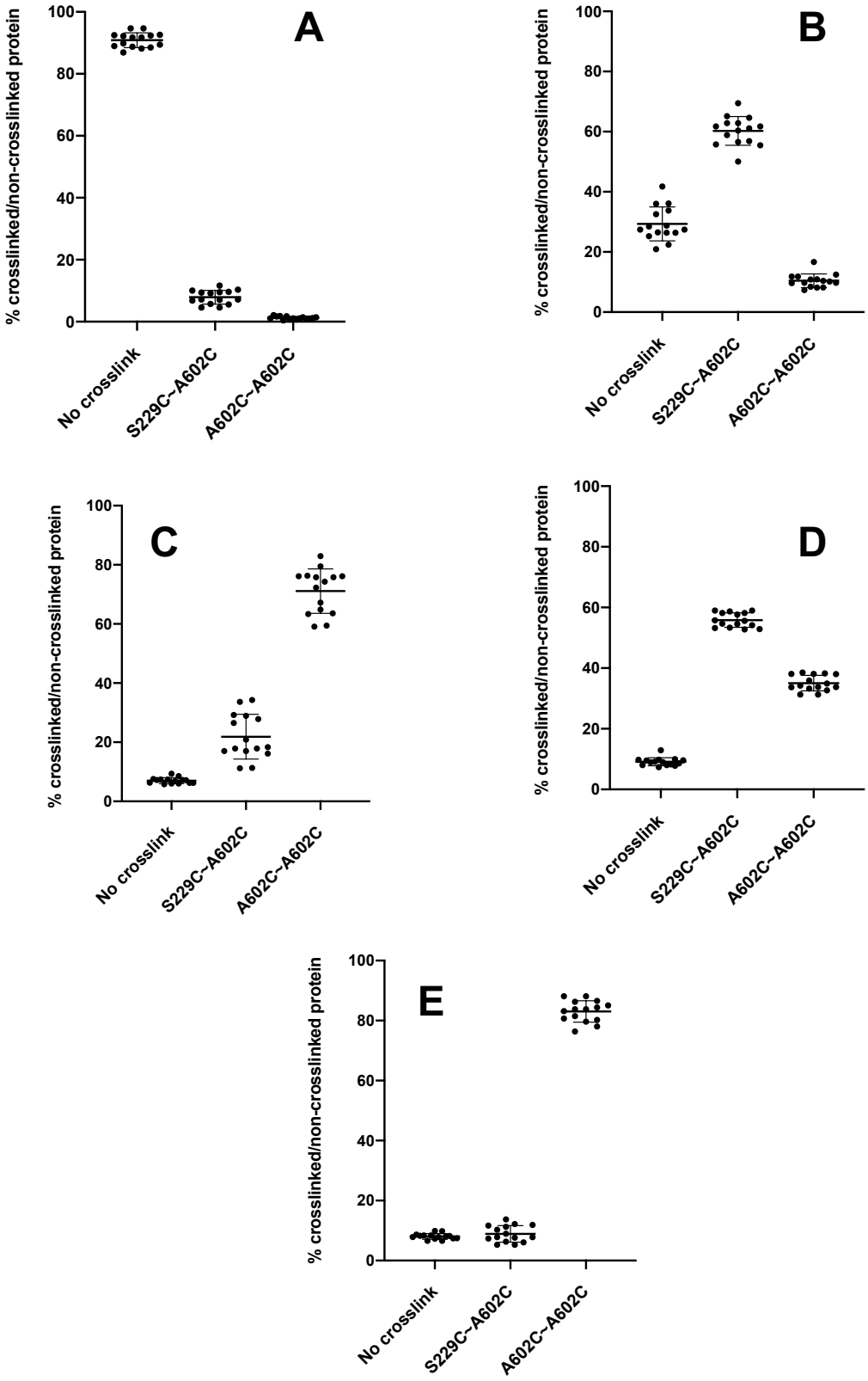
A
% crosslinked/non-crosslinked protein
100
80
60
40
20
0
No crosslink
S229C~A602C
A602C~A602C
B
% crosslinked/non-crosslinked protein
100
80
60
40
20
0
No crosslink
S229C~A602C
A602C~A602C
C
% crosslinked/non-crosslinked protein
100
80
60
40
20
0
No crosslink
S229C~A602C
A602C~A602C
D
% crosslinked/non-crosslinked protein
100
80
60
40
20
0
No crosslink
S229C~A602C
A602C~A602C
E
% crosslinked/non-crosslinked protein
100
80
60
40
20
0
No crosslink
S229C~A602C
A602C~A602C

reactions under the five different conditions mentioned previously. Comparisons in the rate of disulfide bond formation were made individually for each mutant across these five conditions and broadly across the 68 mutants that were used for this study. Surface-exposed and buried as well as proximal and distal cysteines within a LapD dimer were identified based on the Af1503 homology models and the Cβ-Cβ distances obtained from this model (Figure 4.4). SDS-PAGE gels of selected mutants are shown in Figure 4.5A and their corresponding location on the HAMP helices is shown in Figure 4.5B. SDS-PAGE images of all remaining mutants are included in the appendix.

For each lane in the gel, representing each of the five crosslinking conditions, the percentage of protein present in dimerized form was calculated as [dimer/(monomer + dimer)] through densitometric analysis using ImageJ software. Results are summarized in Figure 4.6. For the purpose of this thesis, analysis on all mutants was done with n=1. The tight distribution of the S229C/A602C replicates indicate the robustness of this assay. Further trials will be conducted at a later date, which will enable statistical analysis of the data.

Most mutants showed some level of crosslinking even in the absence of any oxidant. This spontaneous disulfide-bond formation could occur during protein folding or be indicative of the protein sampling conformations in solution where even the more distal residues are able to come into close contact with each other, indicating a level of protein dynamics. Residues L177, M180, V181, A186, I187, F192, T201, P202 and E230 showed the highest levels (>20% of total protein in apo LapD) of disulfide dimer formation in the absence of oxidant. These residues, with the

Figure 4.4. The HAMP domain

A. Sequence alignment of HAMP domains of various proteins. The first four represent LapD homologs from different species.

B. Sequence of the LapD HAMP domain and S-helix with secondary structure modeled after the HAMP domain of Af1503

C. Representation of intra-dimer Cβ-Cβ distances and buried surface area of each HAMP domain residue for the protein Af1503. Yellow represents the A291F variant of Af1503. Residues 189-202 are located on the flexible connector joining the two HAMP helices.

A

```
Pfl_HAMP_S          LRRQLKPLDYMVKQSHAIARREFLSLPDLP-RTPELRRVVLAMNQMVEKLKALFQ 54
PAO1_HAMP_S         LRRQLRPLDQMVRQAHAISRREFLSLPRLP-RTPELRRVVQAMNQMVEKLRTLFA 54
Pput_HAMP_S         LRRQLRPLDYMVEQSHAIARREFLSLPELP-RTPELRRVVQAMNQMVEKLKALFT 54
CdgS9_HAMP_S        LKYLLQPLKRVTAQALAISEHEFPVETKIP-KTPELRQVTLAMNQMVTKVKSLFQ 54
3LNR                HAVAQQRADRIATLLQSFADGQLDTAVGEA-PAPGYERLYDSLRALQRQLREQRA 54
4I3M                HAVAQQRADRIATLLQSFADGQLDTAVGEA-PAPGYERHYDSLRALQRQLREQRA 54
4I44                HAVAQQRADRIATLLQSFADGQLDTAGGEA-PAPGYERLYDSLRALQRQLREQRA 54
2L7H                MSTITRPIIELSNTADKIAEGNLEAEVPHQNRADEIGILAKSIERLRRSLKVAME 55
2L7I                MSTITRPIIELSNTFDKIAEGNLEAEVPHQNRADEIGILAKSIERLRRSLKVAME 55
```

B LapD

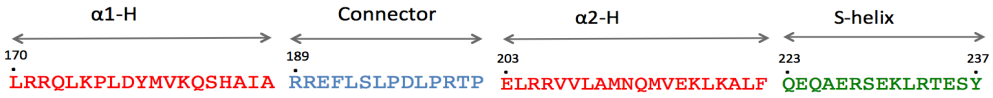

C

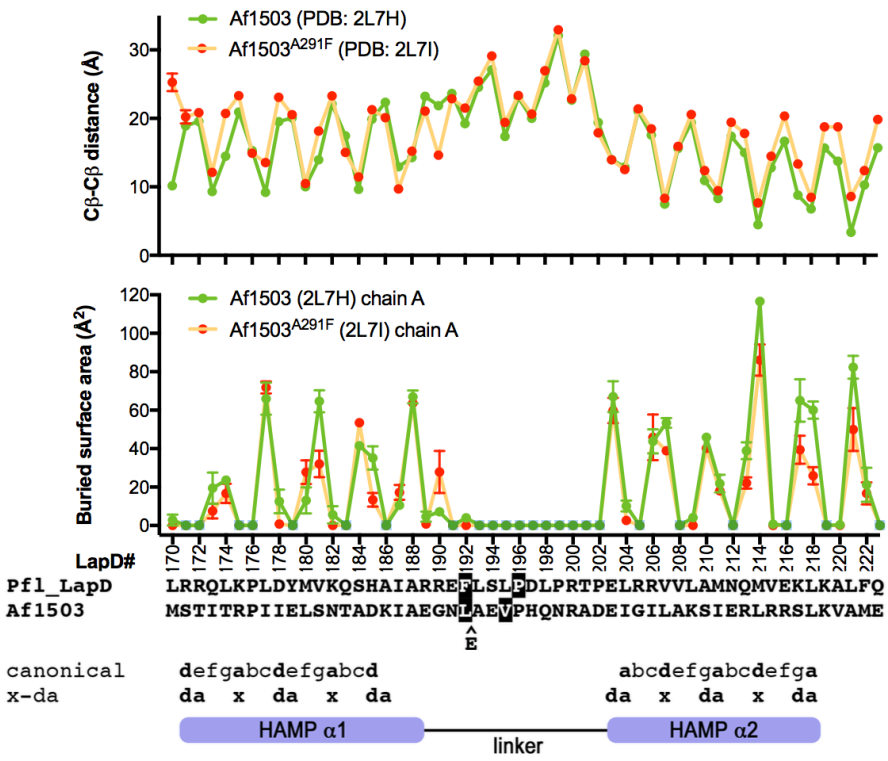

Figure 4.5A. Cysteine crosslinking gels for selected LapD HAMP domain mutants

D178, L174 and N212 are relatively surface exposed and thus show lower extents of disulfide dimer formation as observed from band intensities. L174C and N212C are the only two HAMP domain mutants that show two different crosslinked species of very similar electrophoretic mobilities. These two bands were considered as one for ImageJ analysis.

The S184C mutant shows highest extent of disulfide dimer formation for LapD-c-di-GMP bound protein, and this crosslinking efficiency is lower whenever LapG is present in the system. In contrast, the Q173C mutant shows higher crosslinking efficiencies when c-di-GMP is available, and most mutants in the HAMP domain and S-helix follow this trend.

The L218C mutant is representative of the majority of cysteine mutants located on the α2-H HAMP domain helix and the S-helix in that there is an additional crosslinked species of faster electrophoretic mobility than the main crosslink band in +c-di-GMP states.

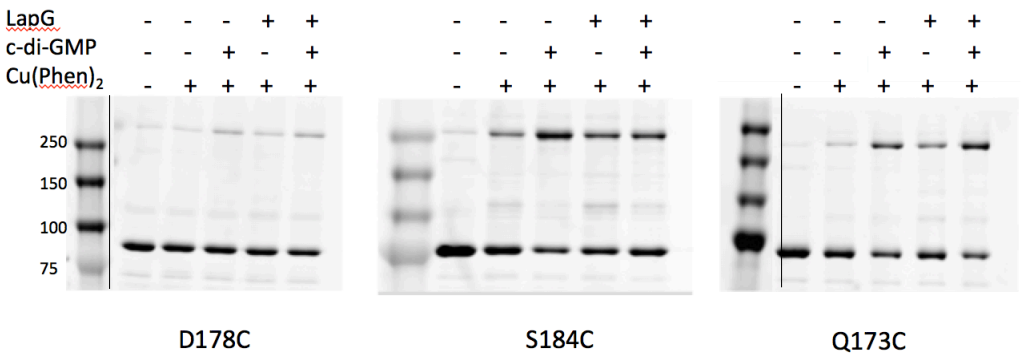
LapG
c-di-GMP
Cu(Phen)2
250
150
100
75
D178C
S184C
Q173C

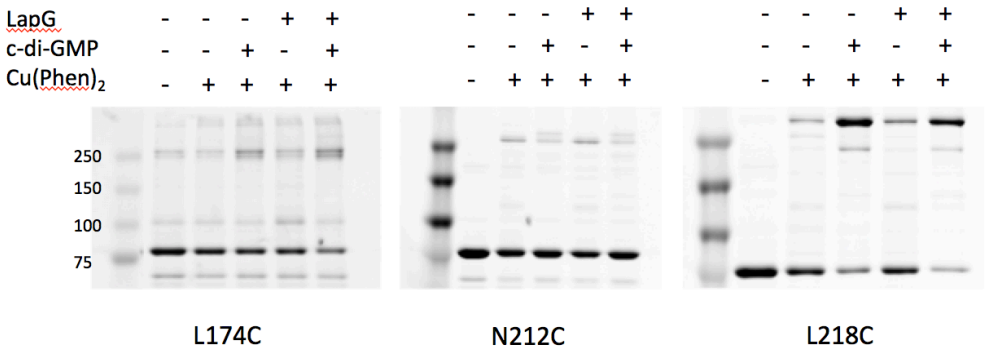
LapG
c-di-GMP
Cu(Phen)2
250
150
100
75
L174C
N212C
L218C

Side view

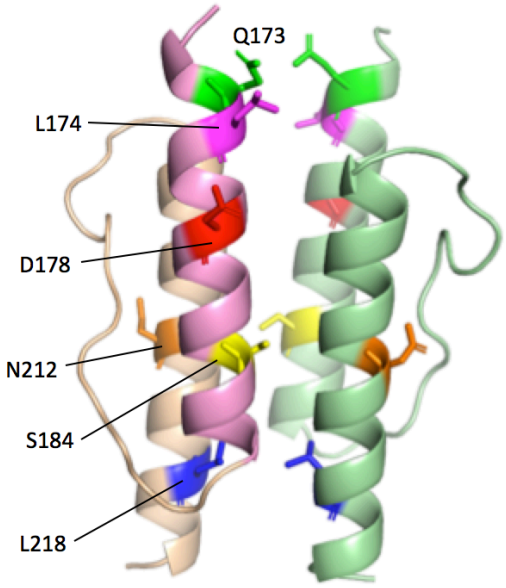

Top view

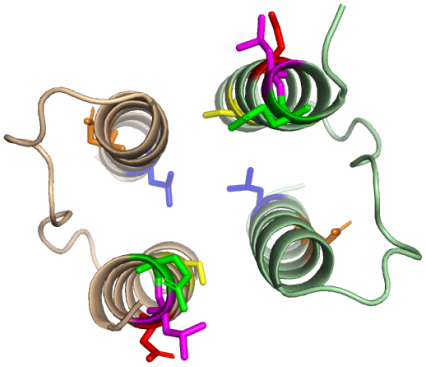

Figure 4.5B. LapD HAMP domain dimers modeled based on available structures of protein Af1503 using the program MODELLER (Fiser and Sali, 2003).

Side and top views of the mutant residues shown in Figure 4.5A are labeled. α1-H (pink) and α2-H (brown) represent the two α-helices of the LapD HAMP domain joined by a flexible connector.

Modeling was done by Dr. Holger Sondermann

Figure 4.6. ImageJ densitometric analysis of HAMP domain and S-helix crosslinks across five different crosslinking conditions.

The percentage of protein crosslinked (disulfide dimer formation: [100*dimer/(monomer + dimer)]) in each lane for each residue mapping the HAMP domain and S-helix was reported.

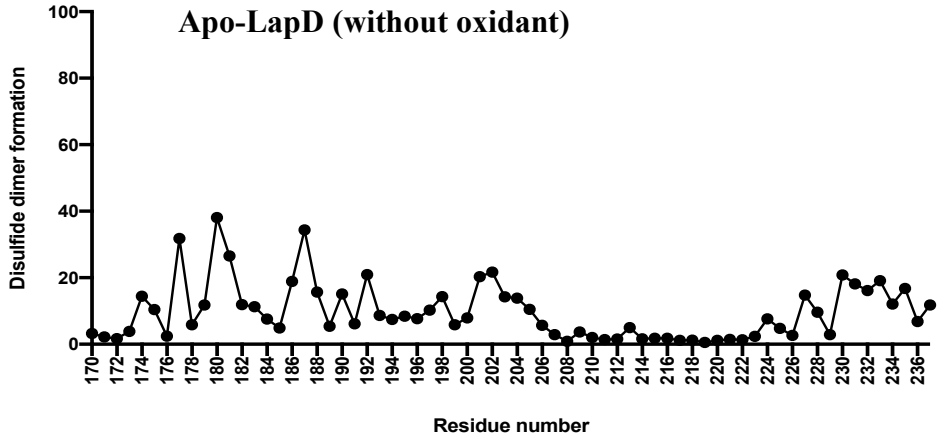
Apo-LapD (without oxidant)
Disulfide dimer formation
Residue number

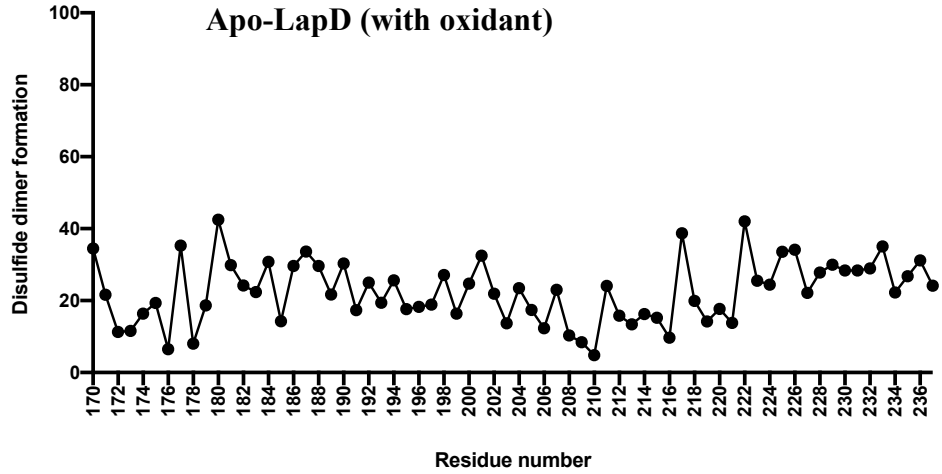
Apo-LapD (with oxidant)
Disulfide dimer formation
Residue number

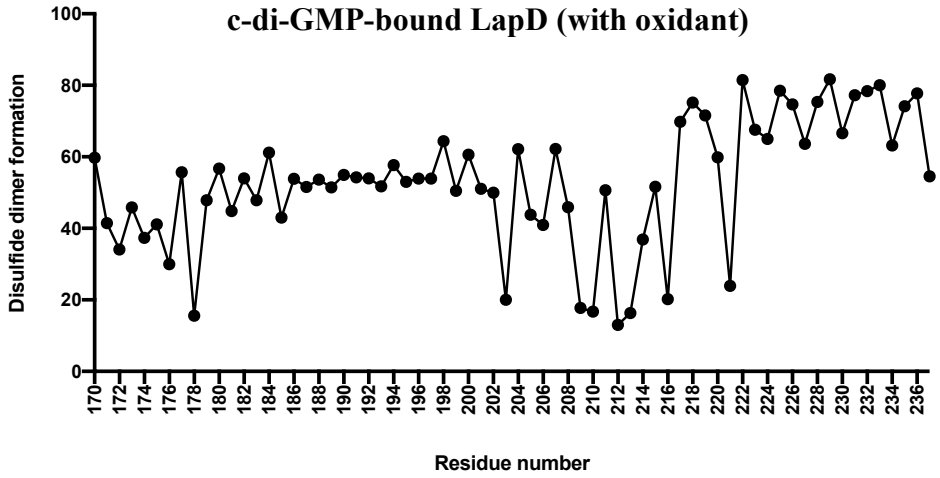
c-di-GMP-bound LapD (with oxidant)
Disulfide dimer formation
Residue number

Figure 4.6. (Continued)

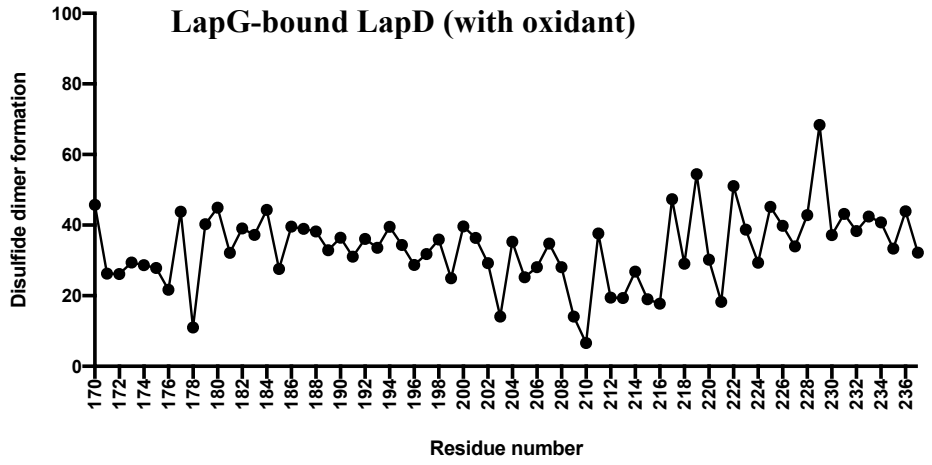

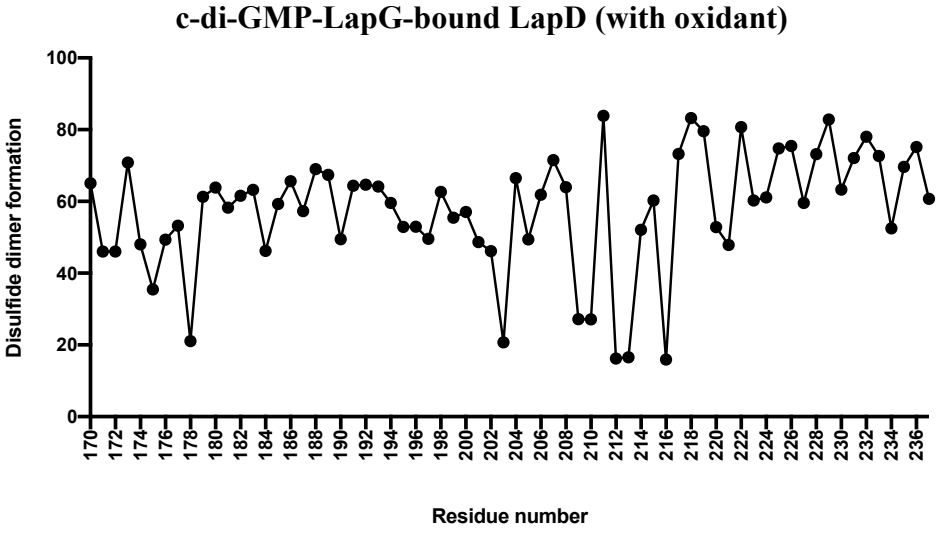

exception of F192, T201, P202 are all located on the first α-helix of LapD's HAMP domain (α1-H). F192, T201, P202 are located on the flexible connector linking the two HAMP helices. In contrast, residues 208-223 showed negligible crosslinking in the absence of oxidant. These residues are located on the second α-helix (α2-H).

For all the HAMP domain mutants generated, relative to apo-LapD, the amount of disulfide bond formation increased in the presence of activators c-di-GMP and LapG, when added independently or in combination with each other. This indicates that the conformational changes occurring during LapD activation bring these residues close enough due to the helical movements to form disulfide bonds. Crosslinking done in the presence of LapG alone for all the mutants progressed at a much lower efficiency than crosslinking done in the presence of c-di-GMP alone. However, crosslinking after LapG incubation was still higher than that observed for apo-LapD. This could be due to the fact that LapG binding to LapD is transient (Chatterjee et al., 2014) and that this signal must be transmitted across the cytoplasmic membrane. Since LapG has a positive effect on crosslinking efficiency, the data corroborate the notion that LapG is a partial activator of LapD in the absence of c-di-GMP.

With few exceptions, most mutants studied here showed a small but noticeable increase in disulfide dimer formation from cysteine crosslinking done on c-di-GMP-bound LapD when compared to crosslinking done in the presence of both c-di-GMP and LapG. These exceptions include the R171C, R190C, Q223C and A200C LapD mutants, which showed a small decrease in the rate of crosslinking. However, further studies are required to confirm this observation through statistical methods using

multiple data sets. The S184C mutant is unique in that it showed a strong decrease in crosslinking whenever LapG was also present in the system.

Another noticeable trend is that cysteine mutants located in the S-helix showed on average higher rates of crosslinking than the HAMP domain mutants. Mutants M211C, K217C, L218C, K219C, F222C, Q225C, A226C, R228C, S229C, K231C, L232C, R233C, S236C showed the highest disulfide-linked dimer formation of >65%.

LapD mutants D178C, E203C, L209C, A210C, N212C, Q213C and E216C showed little crosslinking (<25%). While all these residues are surface exposed, they do not account for all surface exposed residues in the HAMP domain, suggesting that LapD is sufficiently dynamic to allow sampling of more distal residues.

For residues 193-237, crosslinking experiments revealed the existence of an additional disulfide product, which was visualized as a band of faster migration in the gel when compared to the typical cross-linked protein (see Figure 4.5A, mutant L218C for an example). This second population of cross-linked protein was, in most cases, present whenever c-di-GMP was available in the system. These residues are exclusively located in the flexible connector region and the second α-helix (α2-H) of the HAMP domain, and cover the entire S-helix. The formation of LapD dimers-of-dimers occurs when LapD is bound to c-di-GMP (and LapG) (Cooley et al., 2016). This could suggest that the protein forms crosslinks between two LapD dimers in addition to the intra-dimer crosslinks, and it is this crosslink that is visualized on the gel. Proteoliposome-mixing experiments on these mutants could be an approach to test this hypothesis (Cooley et al., 2016).

4.4. Cysteine Crosslinking on LapD Reduced with TCEP Prior to Oxidation

LapD cysteine mutants were treated with the reducing agent tris(2-carboxyethyl)phosphine (TCEP) prior to setting up the crosslinking reactions in order to eliminate the occurrence of spontaneously formed disulfide bonds during expression. TCEP does not contain any thiols and so does not need to be removed prior to performing sulfhydryl-reactive crosslinking reactions. Thus it was preferred over other thiol-containing reducing agents such as dithiothreitol (DTT) and β-mercaptoethanol (β-ME).

TCEP-treated samples did eliminate the presence of cross-linked protein species before incubating with the activators (Figure 4.7). However, it did not reveal any hidden conformational changes that may have been obscured by the presence of an initial large amount of disulfide dimerized protein. The overall trends for each individual mutant between TCEP and non-TCEP treated samples remained the same, with the exception of the M211C mutant. This mutant showed similar crosslinking efficiencies for the c-di-GMP-bound LapD and c-di-GMP-LapG-bound LapD for the TCEP treated sample. However, in non-TCEP treated samples, crosslinking efficiency for c-di-GMP-bound LapD was much lower than that of fully activated c-di-GMP-LapG-bound LapD. Additional trials are required to corroborate if this is an anomaly or experimental outlier. Some mutants also showed a relatively higher rate of disulfide bond formation in TCEP-treated samples, which could not be directly explained by the presence of additional non-crosslinked protein available to undergo conformational changes. A possible reason for this could be that the presence of TCEP reduces the rate of competing reactions producing sulfinic and sulfenic acids

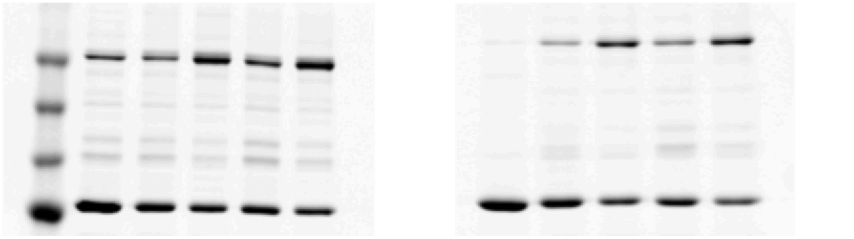

L177C – No TCEP added

L177C – With TCEP added

Figure 4.7. Comparison of TCEP and non-TCEP treated samples.

TCEP reduced disulfide bonds present prior to setting up the crosslinking reactions.

(Careaga and Falke, 1992), thus allowing the LapD disulfide bond formation to occur at a faster rate.

4.5. Cysteine Crosslinking on Periplasmic Output Domain Mutants

Based on the crystal structure of the homologous protein *L. pneumophila* CdgS9, residues from the periplasmic output domain of LapD were chosen for cysteine crosslinking studies (Figure 4.8). In particular, LapD mutants Q37C, H41C, A48C, S52C, P55C and S69C were used for these experiments based on their position in the dimer interface. With the exception of S69C, which is located on the smaller alpha helix (α2-O), these residues are located at different positions along the buried interface of the main alpha helix (α1-O).

Mutant P55C showed highest rates of disulfide dimer formation across all five crosslinking conditions (>75% for all) used. Apart from a slight increase (~1-2%) in crosslinking efficiency in cases where c-di-GMP was available for binding, no significant differences in crosslinking efficiencies were observed among the conditions tested. P55C is located close to the LapG binding site of the periplasmic output domain and is furthest away from the transmembrane (TM) domain. Mutant A48C showed the highest rate of disulfide dimer formation when the protein was incubated with LapG alone. A lower rate of disulfide dimer formation was observed for c-di-GMP-bound LapD, and a further reduction in rate was seen for c-di-GMP-LapG-bound LapD. This could indicate that LapD samples different conformational states when bound to LapG alone than when bound to both LapG and c-di-GMP. Also, despite the transient nature of LapD-LapG binding in the absence of c-di-GMP, this case shows the highest crosslinking efficiency for this mutant.

Figure 4.8. Cysteine crosslinking studies on selected LapD periplasmic domain residues

A. Homology model of *P. fluorescens* LapD periplasmic domain using the corresponding crystal structure *L. pneumophila* CdgS9 as the template showing selected residues used for cysteine crosslinking studies.

B. ImageJ quantification of band intensities.

C. Detection of disulfide dimer formation using in-gel fluorescence.

A

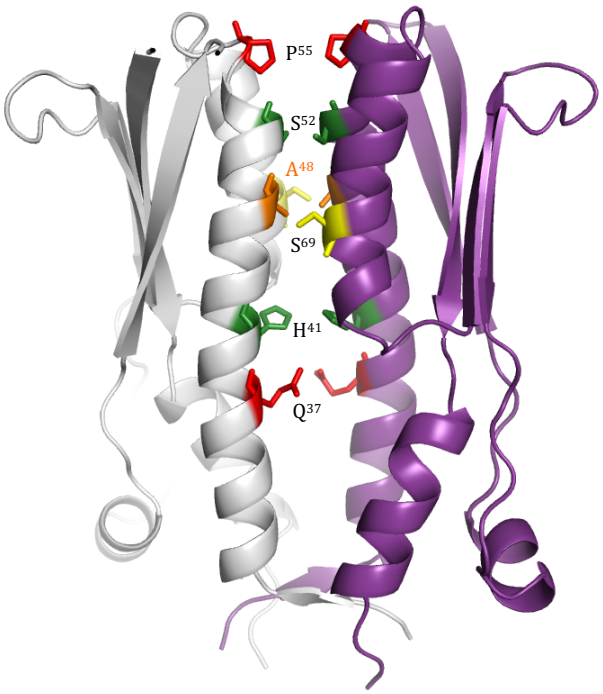
P55
S52
A48
S69
H41
Q37

B

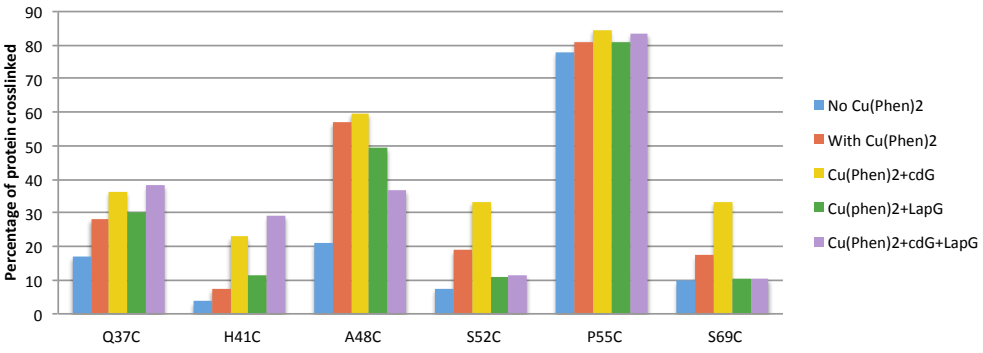
Percentage of protein crosslinked
90
80
70
60
50
40
30
20
10
0
Q37C
H41C
A48C
S52C
P55C
S69C
No Cu(Phen)2
With Cu(Phen)2
Cu(Phen)2+cdG
Cu(phen)2+LapG
Cu(Phen)2+cdG+LapG

Figure 4.8. (Continued)

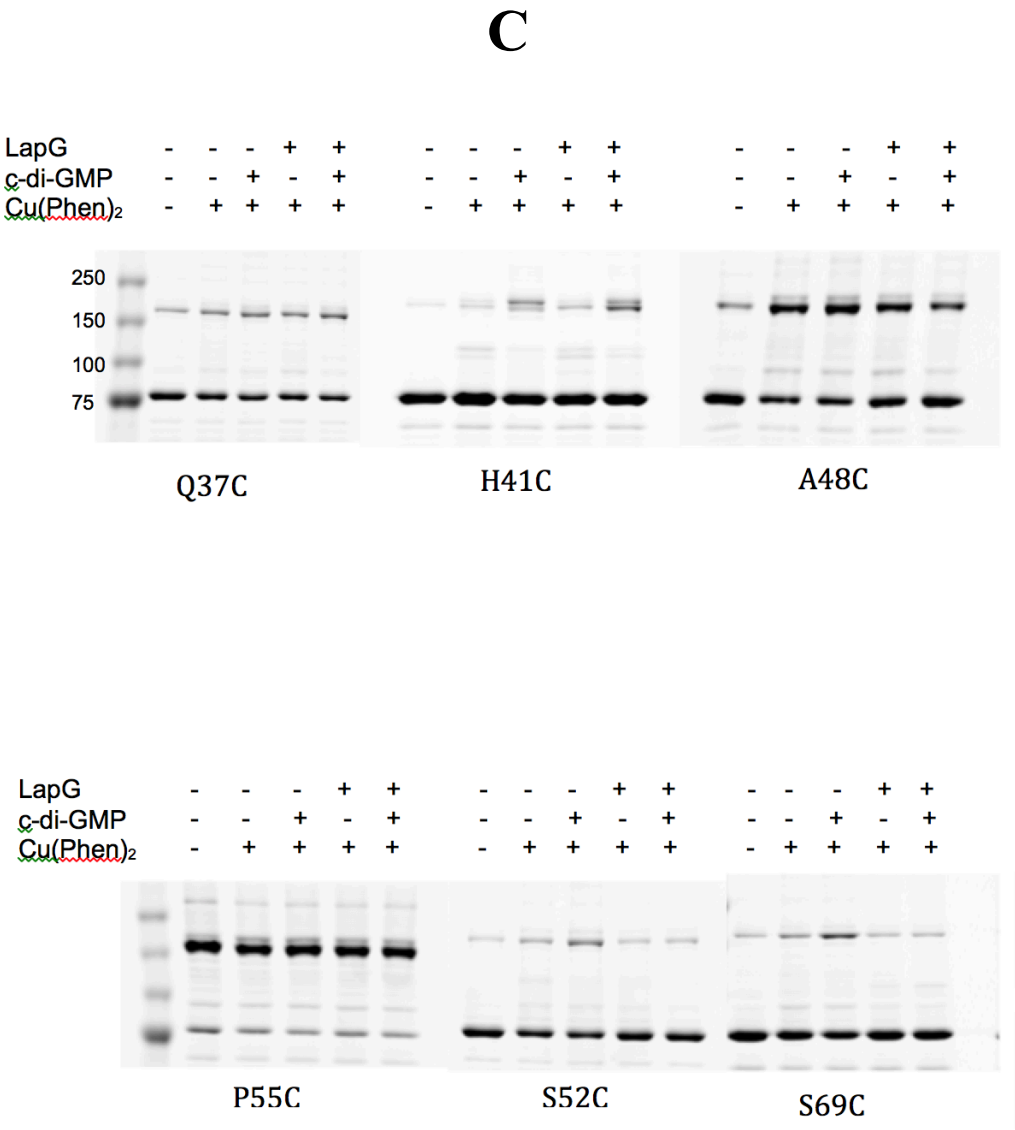

Mutants S52C and S69C showed the highest disulfide dimer formation for LapG-bound LapD. Crosslinking efficiency decreased sharply in the presence of c-di-GMP, and no differences in efficiencies can be observed in c-di-GMP-boundand c-di-GMP-LapG-bound states. In fact, the rate of disulfide dimer formation in the presence of c-di-GMP was even lower than that of apo LapD in the presence of oxidant (which is also true for the A48C mutant). This could imply one of two things: that conformational changes brought about when c-di-GMP is also bound to LapD bring these residues out of close contact with each other; or that the c-di-GMP bound protein is simply less dynamic than apo and LapG-bound protein.

LapD mutants Q37C and H41C showed trends similar to the HAMP domain mutants. The crosslinking efficiency was higher when c-di-GMP was available for binding. These two residues are located near the central region of the output domain and are closer to the transmembrane domain than the other periplasmic domain mutants studied.

4.6. Cysteine Crosslinking on LapD-GcbC Co-expressed Proteins

GcbC is one of the four diguanylate cyclases (DGC; c-di-GMP synthesizing protein) in *P.fluorescens* known to bring about c-di-GMP signaling specificity in the LapA/D/G biofilm effector system. It achieves this signaling specificity through physical interactions with the LapD receptor (Dahlstrom et. al, 2015). Previous studies from the O'Toole laboratory have revealed two motifs that are required for interactions with LapD – a conserved, surface exposed α-helix (Dahlstrom et al., 2015) and the allosteric c-di-GMP binding inhibitory site (I-site) (Dahlstrom et al., 2016). These studies have also shown that GcbC-LapD interactions occur for both

activated- and apo-LapD as well as for catalytically inactive GcbC variants (GGAAF mutants).

We have performed cysteine crosslinking experiments with GcbC-LapD co-expressed proteins (Figure 4.9). This allows us to observe conformational changes in a system closer to physiological conditions and serves as a proof-of concept for the theory that GcbC affects biofilm formation. Rather than adding c-di-GMP exogenously, c-di-GMP is produced by the DGC via its catalytically active GGDEF domain and is always available in this system. Thus the three crosslinking conditions considered (with the exception of the catalytically inactive GcbC mutant, for which apo-LapD should be present instead of c-di-GMP-bound LapD) were: (1) LapD-GcbC without oxidant added, (2) LapD-GcbC with oxidant added, and (3) LapD-LapG-GcbC with oxidant added.

Three variants of GcbC were used: (1) wild-type, (2) GGAAF mutant, and (3) R366E (secondary I-site) mutant. The GGAAF mutation renders GcbC catalytically inactive and unable to produce c-di-GMP. R366 is the only residue in the secondary I-site of GcbC that comes in contact with c-di-GMP. Disrupting this residue has an effect on c-di-GMP binding and GcbC regulation. Dahlstrom et. al. (2016) showed that mutating this residue to glutamic acid prevented the negative-feedback c-di-GMP regulation of GcbC and resulted in the production of c-di-GMP ~16 to 20 times greater than wild-type GcbC. Even though this mutation disrupts interactions between GcbC and LapD, such large increase in c-di-GMP production was found to be sufficient to overcome this loss of interaction and resulted in a ~40% increase in biofilm formation compared to wild-type GcbC.

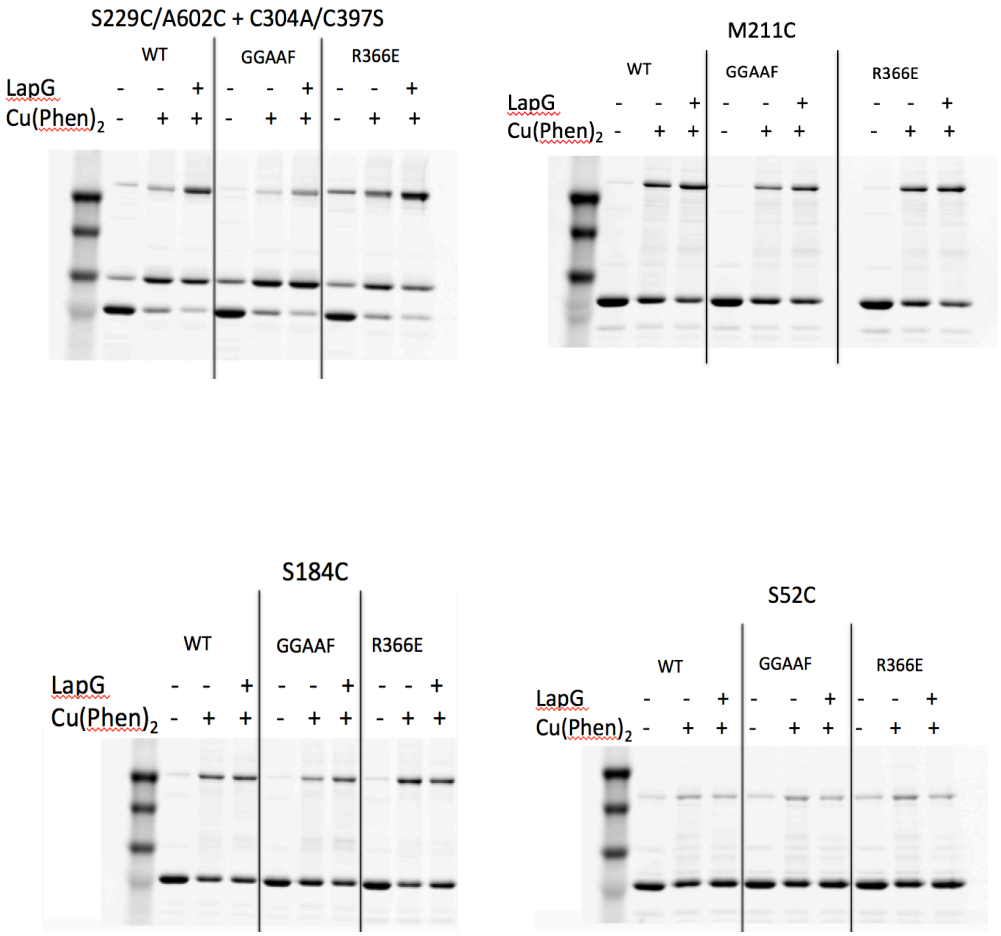

Figure 4.9. Cysteine crosslinking done on co-expressed GcbC-LapD.

Three variants of GcbC were used: wild-type, the catalytically inactive GGAAF mutant, inhibitory site (I-site) mutant R366

LapD-msfGFP mutants S52C from the periplasmic domain, S184C and M211C from the HAMP domain, and the S229C/A602C mutant were chosen for these experiments. These mutants produced visible differences in crosslinking efficiencies across the five crosslinking conditions as seen in the previous experiments done with exogenously added c-di-GMP. To summarize the trends observed from the previous experiments, the S52C and S184C mutants showed a decrease in crosslinking efficiency between the LapD-c-di-GMP bound state and states when LapG is available for binding, while the M211C mutant showed a large increase in crosslinking efficiency for the LapD-c-di-GMP-LapG bound protein. The gels obtained from these experiments were compared with those obtained from crosslinking experiments done in the presence of GcbC instead of c-di-GMP. The results obtained were not as expected. Among the three GcbC variants used, the experiments performed with the GcbC R366E mutant resulted in crosslinking trends most closely matching those of the previous experiments, likely because the larger amount of c-di-GMP produced by this mutant more closely matches the excess c-di-GMP concentrations added during the previous experiments.

S229C/A602C mutant

With wild-type GcbC:

a) No oxidant added: The results obtained closely match those of the previous crosslinking experiments with exogenously added c-di-GMP, with slightly higher amounts of activated protein present (as represented by the A602C~A602C crosslink).

b) Oxidant added: The expected result would be to see a larger quantity of activated c-di-GMP-bound LapD (A602C~A602C crosslink) than the auto-inhibited state (S229C~A602C crosslink). However, this was not the case. The amount of auto-inhibited protein present was comparable to that seen in the previous experiments with apo-LapD. However, there was still an increase in the intensity of the A602C~A602C band (~10%) from apo-LapD, which could imply that c-di-GMP is present in the system, albeit at lower concentrations.

c) Oxidant and LapG added: This led to an increase in the amount of activated protein, with nearly similar amount of activated and auto-inhibited proteins. When compared to previous experiments with exogenously added c-di-GMP, the amount of activated protein in the GcbC experiments was ~25% lower for c-di-GMP-LapG-bound LapD, but was ~15% higher than the LapG-bound LapD. This indicates that c-di-GMP is available in the LapD-GcbC co-expressions, but probably at lower concentrations. Mass-spectroscopy-based c-di-GMP quantification will be required to quantify the amount of c-di-GMP in these samples.

For the catalytically inactive GGAAF variant of GcbC, results closely matched those of the previous experiments with exogenously added c-di-GMP. Small amounts of activated protein were present. This indicates c-di-GMP was not available to bind to LapD, resulting in mostly auto-inhibited protein present in the system.

The M211C LapD mutant followed similar trends to the exogenously added c-di-GMP counterpart. Experiments done with the GGAAF variant of GcbC showed

lower crosslinking efficiencies. Results were inconclusive for the periplasmic domain mutant, S52C. While trends across the three crosslinking conditions were as expected, the crosslinking efficiencies were similar for both wild-type and GGAAF variants of GcbC, while only a slight increase was observed for the R366E mutant.

For the S184C mutant, experiments done with the R366E variant of GcbC most closely match those of the previous experiments. The wild-type GcbC showed comparable crosslinking efficiencies between the first two crosslinking conditions (oxidant added; and oxidant and LapG added), while the GGAAF variant shows an expected lower crosslinking efficiency for the condition where only oxidant was added. Our results indicated that c-di-GMP was available to this system for wild-type GcbC, but likely at lower concentrations than the 25 μM c-di-GMP added exogenously in previous experiments.

In summary, results were rather inconclusive for the GcbC-LapD co-expression crosslinking experiments. The S229C/A602C and the S184C mutant seemed to imply that c-di-GMP was still available to the system as produced by GcbC, but at lower concentrations. Thus, lesser amounts of c-di-GMP-bound LapD were present when compared to the previous experiments. Also, LapD-c-di-GMP binding must take place before cell-lysis, since any c-di-GMP in the cell would likely be washed out during the multiple ultra-centrifugation and resuspension steps involved. The LapD-c-di-GMP binding must also survive the membrane fraction isolation and solubilization steps. These could contribute to lower LapD-c-di-GMP bound protein available for the final crosslinking step. Performing crosslinking experiments directly with the whole cell-lysate or the membrane fraction may reveal more information.

Fluorescent c-di-GMP biosensors can also be used to detect the quantity of c-di-GMP produced within the cell. A potential issue with using cell-lysates is that, on cell-lysis, LapD may not distinguish between the c-di-GMP produced by GcbC from that produced by other DGCs in *E. coli*.

4.7. Distance measurements using Electron Spin Resonance (ESR) – Preliminary Results

Site-directed spin labeling (SDSL) in combination with electron spin resonance [ESR; also known as electron paramagnetic resonance (EPR)] spectroscopy is a useful method to study the structure and conformational dynamics of proteins under conditions close to the physiological state (Altenbach et. al 1998). This technique involves the introduction of a nitroxide spin label at a desired site in a protein. The spin label is introduced by site-directed cysteine mutagenesis on surface exposed residues, followed by the modification of the sulfhydryl group with the nitroxide reagent (Hubbell et al., 1998). Spin labels are unique reporter molecules in that they are paramagnetic and can thus generate an ESR spectrum. Spin labeling allows us to use ESR as a tool to study biomolecules that do not naturally have unpaired electrons.

ESR spectroscopy of spin-labeled molecules can yield a variety of information about the local environment of the spin label: local dynamics of the probe itself, conformational dynamics of protein domains, global protein tumbling (Nesmelov and Thomas, 2010), the nitroxide side-chain mobility, its solvent accessibility, the polarity of its immediate environment, and intramolecular or intermolecular distances ranging from ~8 to 80 Å between two or more nitroxides (Klare, 2013).

We were most interested in distance measurements between two electron spin labels in singly-labeled dimeric LapD. This approach can be used to probe the conformation of the receptor in its active and inactive states. Cysless LapD with a single cysteine substitution was labeled with the commonly used spin-label *S*-(1-oxyl-2,2,5,5-tetramethyl-2,5-dihydro-1H-pyrrol-3-yl)methyl methanesulfonothioate (MTSL). MTSL binds covalently to the cysteine residue present in each monomeric unit of LapD. A pulsed ESR technique, double electron-electron resonance spectroscopy (DEER) was used to measure inter-spin distances. Pulsed EPR techniques can be used to measure distances up to ~80 Å; and up to ~110 Å in fully deuterated systems (Ward et al., 2010) compared to ~20 Å from traditional continuous wave ESR (Steinhoff et. al, 1991). The ESR data can be analyzed as distance distribution plots to generate information on how a specific location in the HAMP domain helices/periplasmic output domain moves relative to its counterpart across the dimer.

Preliminary data for the LapD W125C mutant was obtained. Residue W125, located in the periplasmic output domain is important for LapG binding (Navarro et al., 2011) and was used to study whether detergent solubilized LapD was suitable for ESR experiments. From the available crystal structure of the periplasmic domain of LapD (Navarro et. al, 2011) Cβ-Cβ distances for this residue across the dimer is ~32 Å. The ESR data analyzed by Dr. Peter Borbat as a distance distribution plot revealed a mean distance of ~46 Å, and a peak at 42.3 Å (Figure 4.10). The extra distance could be attributed to the length and flexibility of the spin-labeled side chain. The

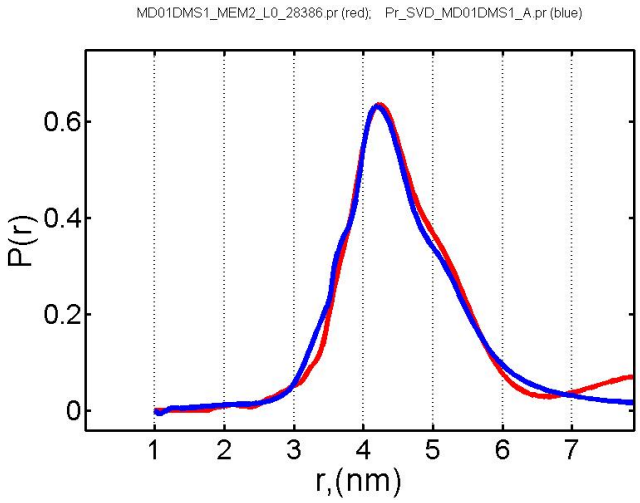

Figure 4.10. Double electron-electron resonance spectroscopy (DEER) distance distribution plot for MTSL-labeled W125C LapD.

The mean intra-dimer distance is ~4.6 nm and the peak at 4.23 nm. From available crystal structure, Cβ- Cβ distance is ~3.2 nm. Reconstruction was done by Tikhonov regularization (red) and singular value decomposition (SVD) (blue).

Data was analyzed by Dr. Peter Borbat

distance between the Cβ atom and the NO group can vary between 4 and 8 Å for MTSSL (Klare, 2013).

Other residues in the HAMP and periplasmic domains will be selected based on the cysteine crosslinking data and available crystal structures and homology models. These mutants will be spin-labeled and analyzed by ESR spectroscopy with the protein in different states of activation: LapG-bound, c-di-GMP-bound, and both LapG-c-di-GMP-bound. This will enable us to distinguish between dynamic and more static states of the protein.

CHAPTER 5

CONCLUSIONS

Although significant progress has been made in understanding the signaling mechanism behind c-di-GMP-mediated biofilm formation in bacteria, much still remains unknown about how the transmembrane receptor LapD transmits conformational changes across the inner membrane. On one hand, LapD is a broadly conserved c-di-GMP effector and has emerged as a paradigm for c-di-GMP signal transmission and specificity. On the other hand, LapD is also an accessible, HAMP-domain-containing protein, enabling the study of the important signaling domain in the context of a full-length receptor. While the HAMP domain has been studied in the context of various chemotaxis proteins and histidine kinase, its function associated with GGDEF (DGC) and EAL (PDE) domains has not been assessed in great detail so far. The present study has employed the method of cysteine crosslinking to map conformational changes of the HAMP domain, S-helix and periplasmic domain of LapD and aims to help gain a better understanding of the regulatory switching mechanism of this HAMP-GGDEF-EAL domain-containing protein.

Results have shown that the majority of LapD cysteine mutants spanning the HAMP domain and S-helix displayed a significant level of intra-dimer crosslinking irrespective of whether they were proximally or distally located in the helices, or whether they were buried or surface-exposed. This indicates the dynamic nature of this protein and suggests that LapD samples multiple conformations in solution such that even more distal residues could come into close contact with each other. The fact that crosslinks were observed in different states of activation of LapD and that the rates of

crosslinking differed across different activation states implies that LapD may operate by oscillating between different bundle conformations. Thus, LapD's signaling mechanism appears to be more consistent with a dynamic bundle model rather than a conventional two-state signaling model such as the gearbox model.

Different crosslinking trends were observed based on the location of the residues on one of the two helices (α1-H and α2-H). Cysteine substitutions made on helix α1-H showed higher levels of crosslinking in the absence of oxidant, whereas residues on helix α2-H showed negligible levels of crosslinking under similar experimental conditions. In partially and fully activated states of LapD, consecutive residues on α2-H showed large differences in disulfide dimer formation, whereas crosslinking efficiencies tended to be more similar for residues belonging to α1-H. Crosslinking gels for residues located on α2-H also revealed the presence of an additional crosslinked species in conditions where the protein was able to form a dimer-of-dimers.

Periplasmic domain mutants located closer to the LapG binding site showed the highest levels of crosslinking for the partially activated LapG-LapD bound protein. Lower rates of crosslinking were observed whenever c-di-GMP was also available for binding. In contrast, for mutants located closer to the transmembrane domain higher crosslinking rates were obtained when c-di-GMP was present in the system.

While still in preliminary stages, ESR spectroscopy promises to be a suitable tool to gain more information about the conformation and dynamics of LapD. Cysteine crosslinking experiments could also be extended to map the periplasmic domain of LapD to reveal different conformations of this domain in different states of

activation of LapD. In conjunction with HAMP domain data, this could reveal much about LapD's activation mechanism.

5.1. Future directions

This study suggests that, rather than adopting few discrete states, the HAMP domain of LapD adopts multiple conformations during signal transduction implying that it adopts a dynamic-bundle model. This work, however, does not give insight into tertiary/quaternary structure elements or how the helices move relative to each other. Electron spin resonance (ESR) spectroscopy could be used to gain more information about the structure and conformational dynamics of LapD. Inter-spin distances of ~8 to 80 Å can be measured using pulsed dipolar ESR, allowing us to distinguish between the dynamic and more static states of LapD. Based on the available structural and cysteine crosslinking data, key residues in the HAMP and periplasmic domains can be selected for ESR spectroscopy. Distance measurements can be obtained between these residues for different states of activation of LapD. Preliminary data from this study have shown that such an approach is feasible for detergent-solubilized LapD. If required, reconstituting LapD in lipid nanodiscs may provide stable protein conformations for such studies.

Cysteine crosslinking could be used to provide structural constraints that can stabilize LapD and make the protein more amenable to crystallographic techniques. Intra-dimer disulfide bonds could also be introduced in the periplasmic, transmembrane or HAMP domains to trap the protein in various conformations and/or reduce flexibility in the more dynamic states of LapD.

Some of the unanswered questions from the crosslinking data could also be looked into. Proteoliposome mixing experiments can confirm whether the presence of the additional crosslinked species in c-di-GMP-bound and c-di-GMP-LapG-bound LapD is indeed due to the formation of LapD dimers-of dimers. Additional periplasmic domain mutants could be generated for cysteine crosslinking studies to reveal more information about the conformational changes occurring in this domain during different states of LapD activation.

Future studies could address how protein-protein interactions control LapD switching and hence provide a mechanism for the apparent signaling specificity in this c-di-GMP sub-network. The results could then be applied to other c-di-GMP dependent processes in the cell. Also, the generality of the conformational switching of LapD could be tested by looking at active DGCs or PDEs containing HAMP domains, which is a common arrangement in this family of proteins.

CHAPTER 6

REFERENCES

Abdel-Aziz SM and Aeron A. 2014. Bacterial biofilm: Dispersal and inhibition strategies. SAJ Biotechnol. 1(1):1-9.

Airola MV, Sukomon N, Samanta D, Borbat PP, Freed JH, Watts KJ, and Crane BR. 2013. HAMP domain conformers that propagate opposite signals in bacterial chemoreceptors. PLOS Biol. 11(2):e1001479. doi:10.1371/journal.pbio.1001479.

Altenbach C, Flitsch SL, Khorana GH, and Hubbell WL. 1998. Structural studies on transmembrane proteins, 2: spin labeling of bacteriorhodopsin mutants at unique cysteines. Biochemistry 28:7806–7812.

Anantharaman V, Balaji S, and Aravind L. 2006. The signaling helix: a common functional theme in diverse signaling proteins. Biology direct. 1:25. doi:10.1186/1745-6150-1-25

Arvind L and Ponting CP. 1999. The cytoplasmic helical linker domain of receptor histidine kinase and methyl-accepting proteins is common to many prokaryotic signaling proteins. FEMS Microbiol. Lett. 176:111-116.

Barends TR, Hartmann E, Griese JJ, Beitlich T, Kirienko NV, Ryjenkov DA, Reinstein J, Shoeman RL, Gomelsky M, Schlichting I. 2009. Structure and mechanism of a bacterial light-regulated cyclic nucleotide phosphodiesterase. Nature 459:1015–1018. doi: 10.1038/nature07966, PMID: 19536266

Bass RB, Butler SL, Chervitz SA, Gloor SL, and Falke JJ. 2007. Use of site-directed cysteine and disulfide chemistry to probe protein structure and dynamics: applications to soluble and transmembrane receptors of bacterial chemotaxis. Meth. Enzymol. 423:25–51. doi:10.1016/S0076-6879(07)23002-2

Bassler BL and Losick R. 2006. Bacterially speaking. Cell 125:237-246.

Becker P, Hufnagle W, Peters G, and Herrmann M. 2001. Detection of different gene expression in biofilm-forming versus planktonic populations of *Staphylococcus aureus* using micro-representational-difference analysis. Appl. Environ. Microbiol. 67:2958-2965.

Boyd CD and O'Toole GA. 2012. Second messenger regulation of biofilm formation: Breakthroughs in understanding c-di-GMP effector systems. Annu. Rev. Cell Dev. Biol. 28:439-462.

Brown MR and Barker J. 1999. Unexplored reservoirs of pathogenic bacteria: Protozoa and biofilms. Trends Microbiol. 7:46-50.

Burmolle M, Ren D, Bjarnsholt T, and Sorensen S. 2014. Interactions in multispecies biofilms: Do they actually matter? Trends in Microbiol. 22(2):84-91.

Camilli A and Bassler BL. 2006. Bacterial small-molecule signaling pathways. Science 311:1113-116.

Capra EJ and Laub MT. 2012. Evolution of two-component signal transduction systems. Annu. Rev. Microbiol. 66:325-347.

Careaga CL and Falke JJ. 1992. Structure and dynamics of *Escherichia coli* chemosensory receptors. Engineered sulfhydryl studies. Biophy. J. 62(1):209–219. doi:10.1016/S0006-3495(92)81806-4.

Characklis WG. 1973. Attached microbial growths. II. Frictional resistance due to microbial slimes. Water Res. 7:1249-1258.

Characklis WG and Marshall KC. 1990. Biofilms. John Wiley, New York.

Caubet R, Pedarros-Caubet F, Chu M, Freye E, de Belem Rodrigues M, Moreau JM, and Ellison WJ. 2004. A radio frequency electric current enhances antibiotic efficacy against bacterial biofilms. Antimicrob. Agents Chemother. 48:4662-4664.

Chatterjee D, Cooley RB, Boyd CD, Mehl RA, O'Toole GA, and Sondermann H. 2014. Mechanistic insight into the conserved allosteric regulation of periplasmic proteolysis by the signaling molecule cyclic-di-GMP. eLife 3:303650. doi:10.7554/eLife.03650.

Chatterjee D. 2013. Structural and biochemical elucidation of the mechanism of c-di-GMP mediated inside-out signaling controlling periplasmic proteolysis. Ph.D. Thesis, Cornell University, Ithaca, NY.

Chervitz SA and Falke JJ. 1996. Molecular mechanism of transmembrane signaling by the aspartate receptor: a model. Proc. Natl. Acad. Sci. (USA) 93:2545–2550. doi:10.1073/pnas.93.6.2545.

Chervitz SA, Lin CM and Falke JJ. 1995. Transmembrane signaling by the aspartate receptor: engineered disulfides reveal static regions of the subunit interface. Biochemistry 34:9722–9733.

Cooley RB, O'Donnell JP, and Sondermann H. 2016. Coincidence detection and bi-directional transmembrane signaling control a bacterial second messenger receptor. eLife 5:e21848. doi:10.7554/eLife.21848.

Costerton JW. 2007. The Biofilm Primar. Springer, Berlin.

Costerton JW, Geesey GG, and Cheng KJ. 1978. How bacteria stick. Sci. Am. 238:86-95.

Costrton JW, Stewart PS, and Greenberg EP. 1999. Bacterial biofilms: A common cause of persistent infections. Science 284:1318-1322.

Dahlstrom KM, Giglio KM, Collins AJ, Sondermann H, and O'Toole GA. 2015. Contributions of physical interactions to signaling specificity between a diguanylate cyclase and its effector. mBio 6:e01978. doi:10.1128/mBio.01978-15.

Dahlstrom KM, Giglio KM, Sondermann H, and O'Toole GA. 2016. The inhibitory site of a diguanylate cyclase is a necessary element for interaction and signaling with an effector protein. J. Bacteriol. 198:1595-1603.

Danese PN, Pratt LA, and Kolter R. 2000. Exopolysaccharide production is required for development of *Escherichia coli* K-12 biofilm architecture. J. Bacteriol. 182:3593-3596.

Daniel L, Vlamakis H, and Kolter R. 2010. Biofilms. Cold Spring Harb. Perspect. Biol. 2:a000398.

Danielson MA, Biemann HP, Koshland DE, and Falke JJ. 1994. Attractant- and disulfide-induced conformational changes in the ligand binding domain of the chemotaxis aspartate receptor: a 19^F NMR study. Biochemistry 33:6100-6109.

Davies DG and Geesey GG. 1995. Regulation of the alginate biosynthesis gene *algC* in *Pseudomonas aeruginosa* during biofilm development in continuous culture. Appl. Environ. Microbiol. 61:860-867.

Davies DG. 2003. Understanding biofilm resistance to antibacterial agents. Nat. Rev. Drug Discov. 2(2):114-122.

Davies DG. 2011. Biofilm dispersion. In Biofilm Highlights, Flemming, H., Wingender, J., and Szewzyk, U. (eds.), pp. 1-28, Springer, Berlin.

Donlan RM. 2002. Biofilms: Microbial life on surfaces. Emerging Infectious Diseases 8(9):881-890.

Dunin-Horkawicz S and Lupas AN. 2010. Comprehensive analysis of HAMP domains: Implications for transmembrane signal transduction. J. Mol. Biol. 397:1156-1174.

Eickhoff MJ and Bassler BL. 2018. Snapshot: Bacterial quorum sensing. Cell 174:1328.

Evans AS. 1978. Causation and disease: A chronological journey. The Thomas Parran Lecture. Amer. J. Epidemiol. 142:1126-1135.

Falke JJ and Hazelbauer GL. 2001. Transmembrane signaling in bacterial chemoreceptors. Trends Biochem. Sci. 26(4):257–265.

Falke JJ and Koshland DE. 1987. Global flexibility in a sensory receptor: A site-directed cross-linking approach. Science 236:1596-1600.

Falke JJ, Sternberg DE, and Koshland DE. 1986. Site-directed sulfhydryl chemistry and spectroscopy: Applications in the aspartate receptor system. Biophys. J. 49:20a.

Ferris HU, Dunin-Horkawicz S, Mondejar LG, Hulko M, Hantke K et al. 2011. The mechanisms of HAMP-mediated signaling in transmembrane receptors. Structure 19:378-385.

Ferris HU, Dunin-Horkawicz S, Hornig N, Hulko M, Martin J, Schultz Joachim E, Zeth K, Lupas AN, and Coles M. 2012. Mechanism of regulation of receptor histidine kinases. Structure 20:56-66.

Fiser A and Sali A. 2003. Modeller: generation and refinement of homology-based protein structure models. Meth. Enzymol. 374:461-491.

Flemming HC. 1998. Relevance of biofilms for the biodeterioration of surfaces of polymeric materials. J. Pol. Degrad. Stab. 59:309-315.

Flemming HC and Wingender J. 2010. Nat. Rev. Microbiol. 8:623-633.

Giacalone D, Smith TJ, Collins AJ, Sondermann H, Koziol LJ, and O'Toole GA. 2018. Ligand-mediated biofilm formation via enhanced physical interaction between a diguanylate cyclase and its receptor. mBio 9:e01254-18. https://doi.org/10.1128/mBio.01254-18.

Giglio KM, Fong JC, Yildiz FH, and Sondermann H. 2013. Structural basis for biofilm formation via the *Vibrio cholerae* matrix protein RbmA. J. Bacteriol. 195:3277-3286.

Goodman AE and Marshall KC. 1995. Genetic responses of bacteria at surfaces. In Microbial Biofilms, J.W. Costerton and H.M. Lappin-Scott (eds.), pp. 80-98, Cambridge University Press, Cambridge, U.K.

Gowrishankar J. 1985. Identification of osmoresponsive genes in *Escherichia coli*: Evidence for participation of potassium and proline transport systems in osmoregulation. J. Bacteriol. 164:434-445.

Gushchin I, Melnikov I, Polovinkin V et al. 2017. Mechanism of transmembrane signaling by sensor histidine kinases. Science 356:6342. eaah6345 doi:10.1126/science.aah6345

Hall-Stoodley L, Costerton JW, and Stoodley P. 2004. Bacterial biofilms: From the natural environment to infectious diseases. Nat. Rev. Microbiol. 2:95-108.

Hazelbauer GL, Falke JJ, and Parkinson JS. 2008. Bacterial chemoreceptors. High-performance signaling in networked arrays. Trends Biochem. Sci. 33:9-19.

Henrici AT. 1933. Studies of freshwater bacteria. I. A direct microscopic technique. J. Bacteriol. 25:277-287.

Hentzer M, Teitzel GM, Balzer GJ, Heydorn A, Molin S, Givskov M, and Parsek MR. 2001. Alginate overproduction affects *Pseudomonas aeruginosa* biofilm structure and function. J. Bacteriol. 183:5395-5401.

Heukelekian H and Heller A. 1940. Relation between food concentration and surface for bacterial growth. J. Bacteriol. 40(4):547-558.

Hinsa SM, Espinosa-Urgel M, Ramos JL, and O'Toole GA. 2003. Transition from reversible to irreversible attachment during biofilm formation by *Pseudomonas fluorescens* WCS365 requires an ABC transporter and a large secreted protein. Mol. Microbiol. 49:905-918.

Hinsa SM and O'Toole GA. 2006. Biofilm formation by *Pseudomonas fluorescens* WCS365: a role for LapD. Microbiol. Mol. Biol. Rev. 66:373-395.

Hoiby N. 2017. A short history of microbial biofilms and biofilm infections. APMIS 125:272-275.

Hoiby N, Flensborg E, Beck B Friis B, Jacobsen S, and Jacobsen L. 1977. *Pseudomonas aeruginosa* infection in cystic fibrosis. Diagnostic and prognostic significance of *Pseudomonas aeruginosa* precipitins determined by means of crossed immunoelectrophoresis. Scand. J. Respir. Dis. 58(2):65-79.

Hubbell WL, Gross A, Langen R, and Lietzow MA. 1998. Recent advances in site-directed spin labeling of proteins. Curr. Opin. Struct. Biol. 8:649-656.

Huges KA, Sutherland IW, and Jones MV. 1998. Biofilm susceptibility to bacteriophase attack: the role of phage-borne polysaccharide depolymerase. Microbiology 144:3039-3047.

Hughson, A. G., & Hazelbauer, G. L. (1996). Detecting the conformational change of transmembrane signaling in a bacterial chemoreceptor by measuring effects on disulfide cross-linking in vivo. Proc. Natl. Acad. Sci. (USA) 21:11546–11551. doi:10.1073/pnas.93.21.11546

Hulko M, Berndt F, Gruber M, Linder, JU, Truffault V, Schultz A, Martin J, Schultz JE, Lupas AN, and Coles M. 2006. The HAMP domain structure implies helix rotation in transmembrane signaling. Cell 126:929-940.

Jamal M, Tasneem U, Hussain T, and Andleeb S. 2015. Bacterial biofilm: Its composition, formation and role in human infections. RRJMB 4(3):1-14.

Jefferson KK. 2004. What drives bacteria to produce a biofilm? FEMS Microbiology Letters 236:163-173.

Jones CJ, Utada A, Davis KR et al. 2015. C-di-GMP regulates motile to sessile transition by modulating MshA pili biogenesis and near-surface motility behavior in *Vibrio cholerae*. PLOS Pathog. 11(10):e1005068. doi:10.1371/journal. Ppat. 1005068.

Kanematsu H and Barry DM. 2005. Biofilm and Material Science. Springer Cham, Heidelberg, Germany,

Khursigara, CM, Wu X, Zhang, P, Lefman J, and Subramaniam S. 2008. Role of HAMP domains in chemotaxis signaling by bacterial chemoreceptors. Proc. Natl. Acad. Sci. (USA) 105:16555–16560. doi:10.1073/pnas.0806401105

Kirmusaoglu S. 2016. Staphylococcal biofilms: Pathogenicity, mechanism and regulation of biofilm formation by quorum-sensing systems and antibiotic resistance mechanisms of biofilm-embedded microorganisms. In Microbial Biofilms: Importance and Applications, eds. D Dhanasekaran and N. Thajuddin, IntechOpen, pp. 189-207. http://dx.doi.org/10.5772/62943.

Klare J. 2013. Site-directed spin labeling EPR spectroscopy in protein research. Biol. Chem. 394:1281-1300.

Krell T, Lacal J, Busch A, Silva-Jimenez H, Guazzaroni M-E, and Ramos JL. 2010. Bacterial sensor sinases: Diversity in the secognition of environmental signals. Annu. Rev. Microbiol. 64:539-559.

Kumita H, Yamada S, Nakamura H, and Shiro Y. 2003. Chimeric sensory kinases containing O2 sensor domain of FixL and histidine kinase domain from thermophile. Biochim. Biophys. Acta 1646:136-144.

Lappin-Scott H, Burton S, and Stoodley P. 2014. Revealing a world of biofilms – the pioneering research of Bill Costerton. Nature Rev Microbiol. AOP, published online 26 August 2014; doi:10.1038/nrmicro3343.

Lewis K. 2005. Persister cells and the riddle of biofilm survival. Biochemistry 70:267-274.

Lister PD, Wolter DJ, and Hanson ND. 2009. Antibacterial-resistant *Pseudomonas aeruginosa*: Clinical impact and compact regulation of chromosomally encoded resistance mechanisms. Clin. Microbiol. Rev. 22:582-610.

Lopez D, Vlamakis H, and Kolter R. 2010. Biofilms. Cold Spring Harb. Perspect. Biol. 2:a000398.

Mah TF and O'Toole, G.A. 2001. Mechanisms of biofilm resistance to antimicrobial agents. Trends in Microbiology 9(1):34-39.

Matamouros S, Hager KR, and Miller SI. 2015. HAMP domain rotation and tilting movements associated with signal transduction in the PhoQ sensor kinase. mBio 6(3);e00616-15. doi:10.1128/mbio.00616-15.

Melo LF and Bott TR 1997. Biofouling in water systems. Exp. Therm. Fluid Sci. 14:375-381.

Milburn MV, Prive GG, Milligan DL, Scott WG, Yeh J, Jancarik J, Koshland DE, and Kim SH. 1991. Three-dimensional structures of the ligand-binding domain of the bacterial aspartate receptor with and without a ligand. Science 254:1342-1347.

Mittelman MW. 1996. Biological fouling of purified water systems: Part 3: Treatment. Microcontamination 4(1):30-40.

Monds RD and O'Toole GA. 2009. The developmental model of microbial biofilms: ten years of a paradigm up for review. Trends Microbiol: 17(2):73-87.

Navarro MV, Newell PD, Krasteva PV, Chatterjee D, Madden DR, O'Toole GA, and Sondermann H. 2011. Structural basis for c-di-GMP-mediated inside-out signaling controlling periplasmic proteolysis. PLOS Biol. 9:e1000588. doi. 10.1371/journal.pbio.1000588.

Nesmelov YE and Thomas DD. 2010. Protein structural dynamics revealed by site-directed spin labeling and multifrequency EPR. Biophys. Rev. 2(2), 91–99. doi:10.1007/s12551-010-0032-5

Newell PD, Monds RD, and O'Toole GA 2009. LapD is a bis-(3'5')-cyclic dimeric GMP-binding protein that regulates surface attachment by *Pseudomonas fluorescens* PF0-1. Proc. Natl. Acad. Sci. USA 106:3461-3466.

Newell PD, Yoshioka S, Hvorecny KL, Monds RD, and O'Toole GA. 2011. Systematic analysis of diguanylate cyclases that promote biofilm formation *Pseudomonas fluorescens* PfO-1. J. Bacteriol. 193:4685-4698.

NINS. 1998. National Nosocomial Infections Surveillance (NNIS) System Report, data summary from October 1986 to April 1998, issued June 1998. Am. J. Infect. Control 26:522-533.

O'Toole GA, Kaplan HB and Koilter R. 2000. Biofilm formation as microbial development. Annu. Rev. Microbiol. 54:49-79.

O'Toole GA and Kolter R. 1998a. Flagellar and twitching motility are necessary for *Pseudomonas aeruginosa* biofilm development. Mol. Microbiol. 30:295-304.

O'Toole GA and Kolter R. 1998b. Initiationof biofilm formation in *Pseudomonas fluorescens* WCS365 proceeds via multiple, convergent signaling pathways: a genetic analysis. Mol. Microbiol. 28:449-461.

Paraje M. 2011. Antimicrobial resistance in biofilms. Science against microbial pathogens: Communicating current research and technological advances. A. Mendez-Vilas (Ed.), FORMATEX.

Parkinson JS. 2010. Signaling mechanisms of HAMP domains in chemoreceptors and sensor kinases. Annu. Rev. Microbiol. 64:101-122.

Petrova OE, and Sauer K. 2016. Escaping the biofilm in more than one way: desorption, detachment or dispersion. Current Opinion Microbiol. 30:67-78.

Prakash B, Veeregowdda BM, and Krishnappa G. 2003. Biofilms: A survival strategy of bacteria. J. Curr. Sci. 85:1299-1307.

Pratt LA and Kolter R. 1998. Genetic analysis of *Escherichia coli* biofilm formation: Roles of flagella, motility, chemotaxis and type I pili. Mol. Microbiol. 30:285-293.

Prignet-Combaret PC, Vidal O, Dorel C, and Lejeune P. 1999. Abiotic surface sensing and biofilm-dependent regulation of gene expression in *Escherichia coli*. J. Bacteriol. 181:5993-6002.

Rabin N, Zheng Y, Opoku-Temeng C, Du Y, Bonsu E, and Sintim HO. 2015. Biofilm formation mechanisms and targets for developing antibiofilm agents. Future Med. Chem. 7(4):493-512.

Rabin N. Zheng Y, Opoku-Temeng C, Du Y, Bonsu E, and Sintim HO. 2015. Biofilm formation mechanisms and targets for developing antibiofilm agents. Future Med. Chem. 7(4):493-512.

Rao F, Yang Y, Qi Y, and Liang Z. 2008. Catalytic mechanism of cyclic di-GMP-specific phosphodiesterase: A study of the EAL domain-containing RocR from *Pseudomonas aeruginosa*. J. Bacteriol. 190:3622-3631.

Rediske AM, Roeder BL, Nelson JL, Robison RL, Schaalje GB, Robison RA, and Pitt WG. 2000. Pulsed ultrasound enhances the killing of *Escherichia coli* biofilms by aminoglycoside antibiotics in vivo. Antimicrob. Agents Chemother. 44:771-772.

Rochex A and Lebeault JM. 2007. Effects of nutrients on biofilm formation and detachment of a *Pseudomonas putida* strain isolated from a paper machine. Water Res. 41:2885-2892.

Romling U, Galperin MY, and Gomelsky M. 2013. Cyclic di-GMP: the first 25 years of a universal bacterial second messenger. Microbiol. Mol. Biol. Rev. 77:1-52.

Ross P, Weinhouse H, Aloni Y, Michaeli D, Weinberger-Ohana P, Mayer R, Braun S, de Vroom E, van der Marel GA, van Boom JH, and Benziman M. 1987. Regulation of cellulose synthesis in *Acetobacter xylinum* by cyclic diguanylic acid. Nature 325:279-281.

Ryan RP, Fouhy Y, Lucey JF, Crossman LC, Spiro S, He Y-W, Zhang L.-H, Heeb S, Camara M, Williams P and Dow JM. 2006. Cell-cell signaling in *Xanthomonas campestris* involves an HD-GYP domain protein that functions in cyclic di-GMP turnover. Proc. Natl. Acad. Sci. USA 103:6712-6717.

Sauer K, Camper AK, Ehrlich GD, Costerton JW, and Davies DG. 2002. *Pseudomonas aeruginosa* displays multiple phenotypes during development as a biofilm. J. Bacteriol. 184:1140-1154.

Sledjeski DD and Gottesman S. 1996. Osmotic shock induction of capsule synthesis in *Escherichia coli* K-12. J. Bacteriol. 178:1204-1206.

Sondermann H, Shikuma NJ and Yildiz FH. 2012. You've come a long way:c-di-GMP signaling. Curr. Opinion Microbiol. 15:140-146.

Steinhoff HJ, Dombrowsky O, Karim C, and Schneiderhahn C. 1991. Two-dimensional diffusion of small molecules on protein surfaces: an EPR study of the restricted translational diffusion of protein-bound spin labels. Eur. Biophys. Lett. *20*, 293–303.

Stock AM, Robinson VL, and Goudreau PN. 2000. Two-component signal transduction. Annu. Rev. Biochem. 69:183-215.

Sundriyal A, Massa C, Samoray D, Zehender F, Sharpe T, Jenal U, and Schirmer T. 2014. Inherent regulation of EAL domain-catalyzed hydrolysis of second messenger cyclic di-GMP. Journal of Biological Chemistry 289:6978– 6990. doi:10.1074/jbc.M113.516195, PMID: 24451384

Swain KE & Falke JJ. 2007. Structure of the conserved HAMP domain in an intact, membrane-bound chemoreceptor: a disulfide mapping study. Biochemistry 46:13684–13695. doi:10.1021/bi701832b

Teschler JK, Zamorano-Sanchez D, Utada AS et al. 2015. Living in the matrix: assembly and control of *Vibrio cholerae* biofilms. Nat. rev. Microbiol. 13(5):255-268.

Tolker-Nielsen T. 2014. *Pseudomonas aeruginosa* biofilm infections: From molecular biofilm biology to new treatment possibilities. APMIS 122 (Suppl. 138):1-51.

Valentini M and Filloux A. 2016. Biofilms and cyclic-di-GMP (c-di-GMP) signaling: Lessons from *Pseudomonas aeruginosa* and other bacteria. J. Biol. Chem. 291:12547-12555.

Valentini M and Filloux A. 2016. Biofilms and cyclic-di-GMP (c-di-GMP) signaling: Lessons from *Pseudomonas aeruginosa* and other bacteria. J. Biol. Chem. 291:12547-12555.

Ward SM, Bormans AF and Manson MD. 2006. Mutationally altered signal output in the Nart (NarX-Tar) hybrid chemoreceptor. J. Bacteriol. 188:3944-3951.

Ward R, Bowman A, Sozudogru E, El-Mkami H, Owen-Hughes T, and Norman DG. 2010. EPR distance measurements in deuterated proteins. J. Magn. Reson. *207*, 164-167.

Watnick PI and Kolter R. 1999. Steps in the development of a *Vibrio cholera* E1 Tor biofilm. Mol. Microbiol. 34:586-595.

Williams SB and Stewart V. 1999. MicroReview: Functional similarities among two-component sensors and methyl-accepting chemotaxis proteins suggest a role for linker region amphipathic helices in transmembrane signal transduction. Mol. Microbiol. 33: 1093-1102. doi:10.1046/j.1365-2958.1999.01562.x

Wingender J, Neu TR and Flemming HC. 1999. Microbial extracellular polymeric substances. Springer Verlag, Berlin, pp. 1-19.

Xavier, J.B., Picioreanu, C., Rani, S.A., van Loosdrecht, M.C.M., and Stewart, P.S. 2005. Biofilm-control strategies based on enzymic disruption of the extracellular polymeric substance matrix: A modeling study. Microbiology 151:3817-3832.

Yeh JI, Biemann HP, Prive GG, Pandit J, Koshland DE, Kim SH. 1996. High resolution structures of the ligand binding domain of the wild type bacterial aspartate receptor. J. Mol. Biol. 262:186–201

Yildiz FH and Visick KL. 2009. Vibrio biofilms: so much the same yet so different. Trends Microbiol. 17(3):109-118. doi:10.1016/j.tim.2008.12.004.

Zhou Q, Ames P and Parkinson JS. 2009. Mutational analyses of HAMP helices suggest a dynamic bundle model of input-output signalling in chemoreceptors. Mol. Microbiol. 73(5), 801–814. doi:10.1111/j.1365-2958.2009.06819.x

Zobel CE. 1943. The effect of solid surfaces upon bacterial activity. J. Bacteriol. 46:39-56.

APPENDIX

Cysteine crosslinking gels for all HAMP domain and S-helix mutants are shown here. Residue numbers are mentioned below each gel. Samples loaded in each lane of the gel are as follows:

- Lane 1: Molecular weight markers
- Lane 2: Apo-LapD without oxidant
- Lane 3: Apo-LapD with oxidant
- Lane 4: c-di-GMP-bound LapD with oxidant
- Lane 5: LapG-bound LapD with oxidant
- Lane 6: c-di-GMP-LapG-bound LapD with oxidant

Samples used for these gels were not treated with TCEP prior to oxidation.

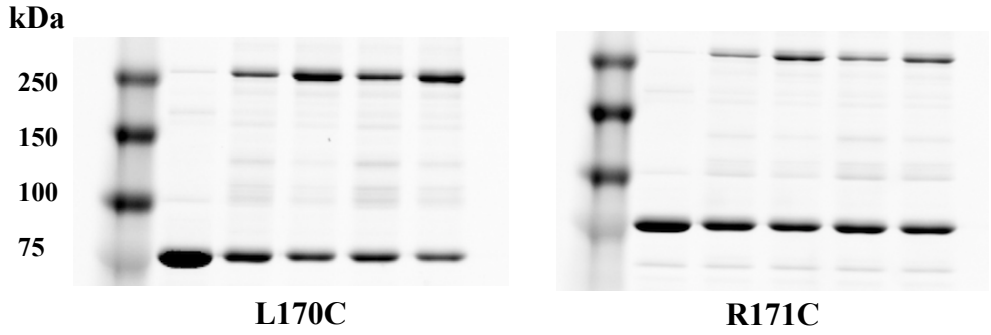
kDa
250
150
100
75
L170C
R171C

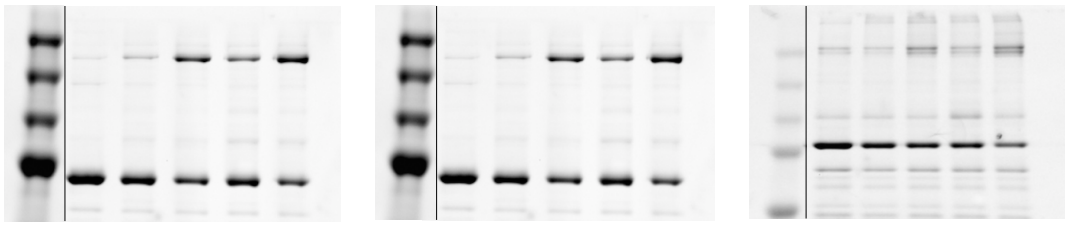
R172C
Q173C
L174C

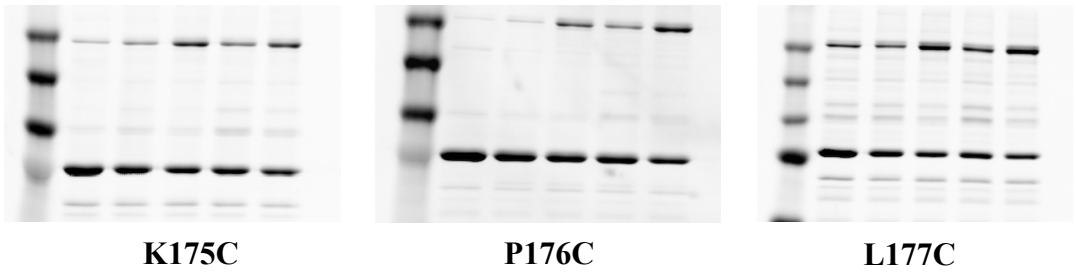
K175C
P176C
L177C

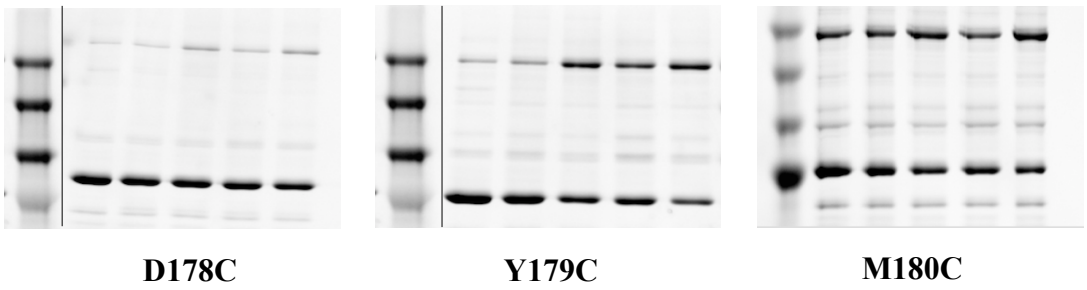
D178C
Y179C
M180C

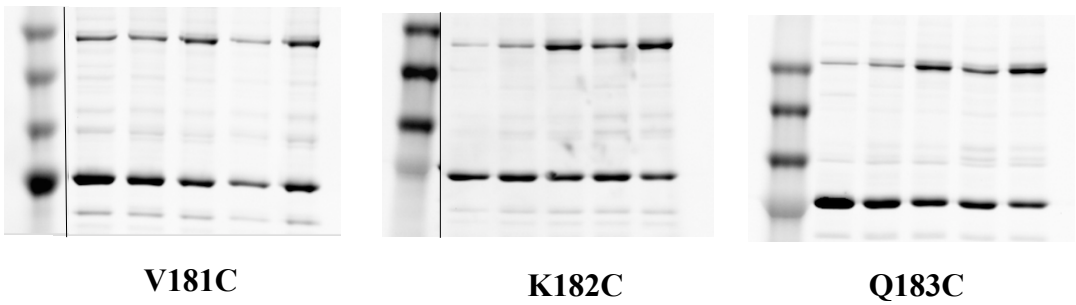
V181C
K182C
Q183C

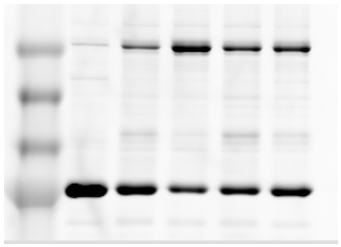

S184C

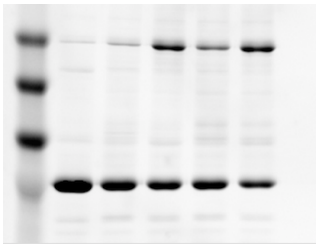

H185C

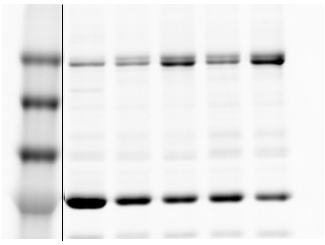

A186C

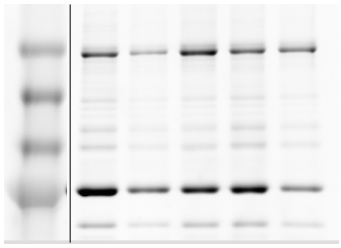

I187C

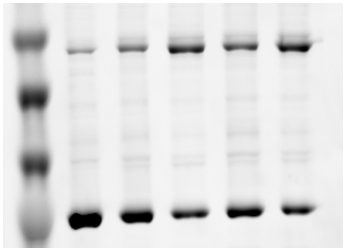

A188C

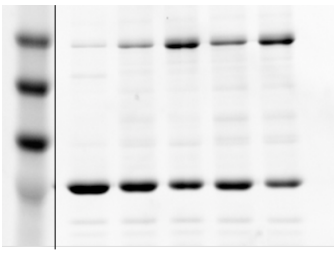

R189C

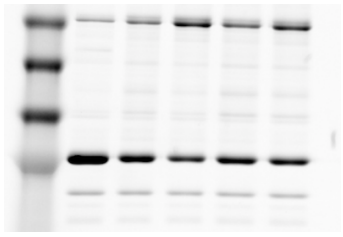

R190C

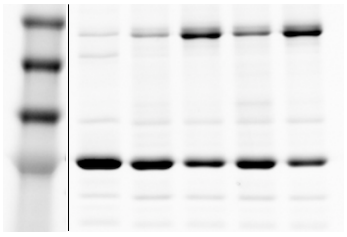

E191C

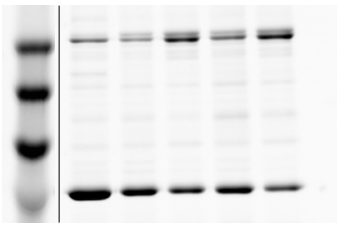

F192C

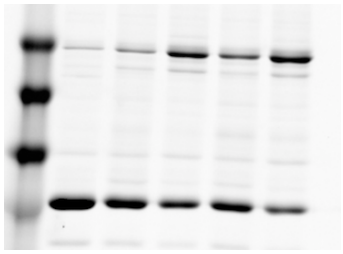

L193C

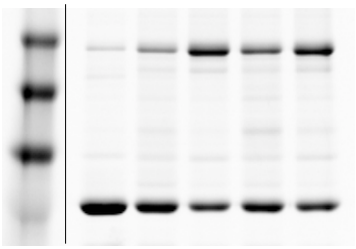

S194C

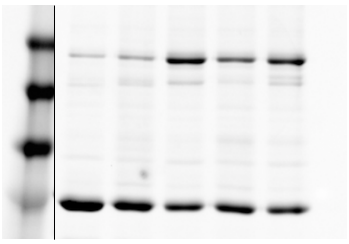

L195C

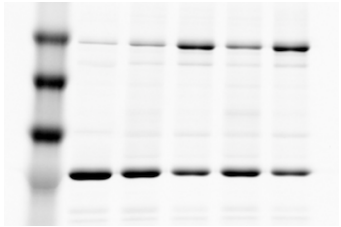

P196C

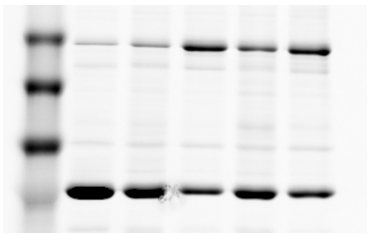

D197C

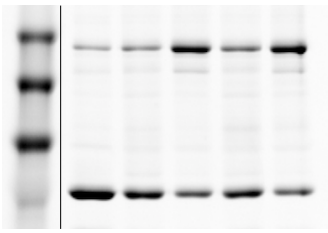

L198C

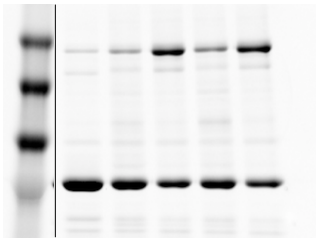

P199C

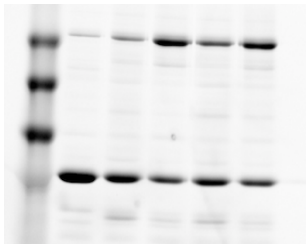

R200C

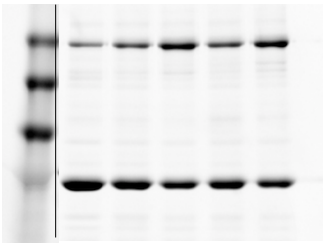

T201C

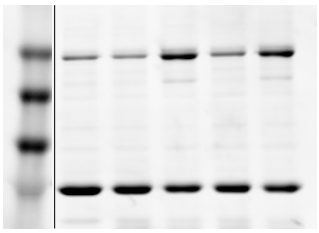

P202C

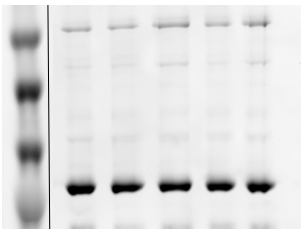

E203C

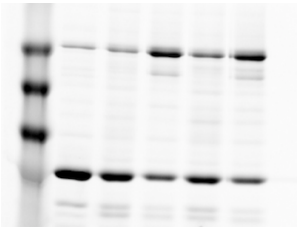

L204C

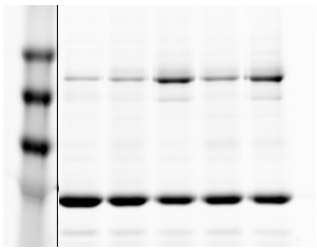

R205C

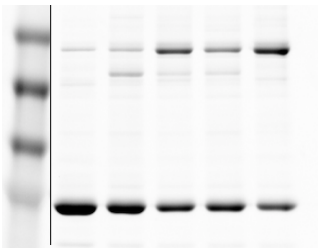

R206C

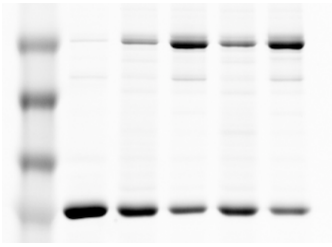

V207C

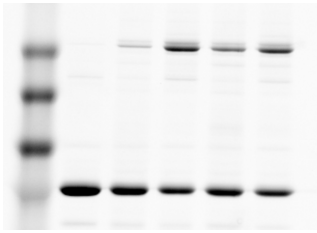

V208C

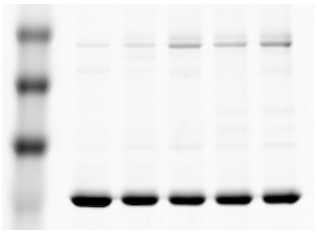

L209C

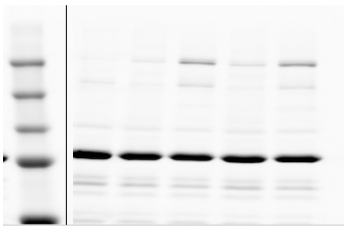

A210C

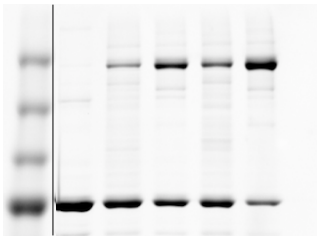

M211C

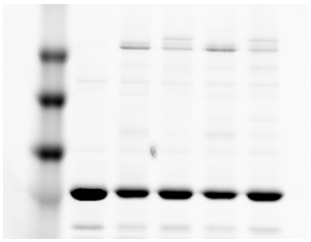

N212C

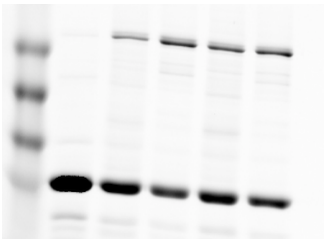

M214C

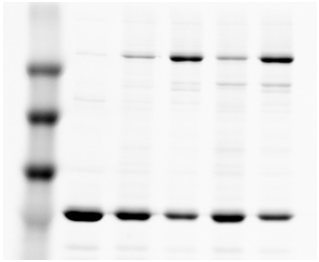

V215C

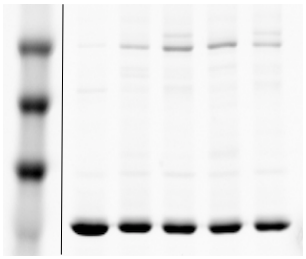

E216C

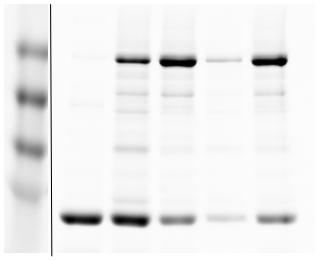

K217C

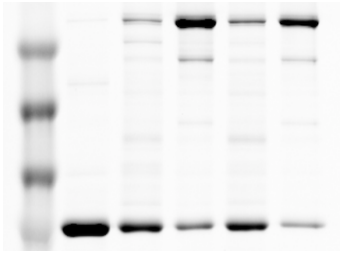

L218C

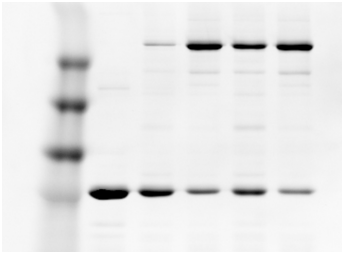

K219C

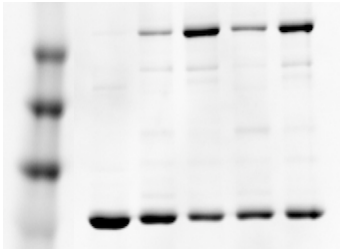

A220C

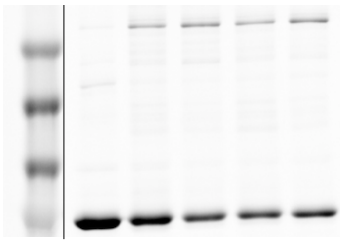

L221C

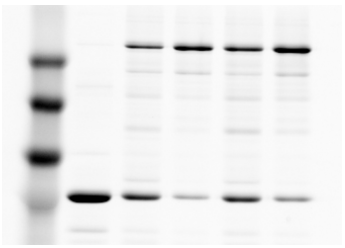

F222C

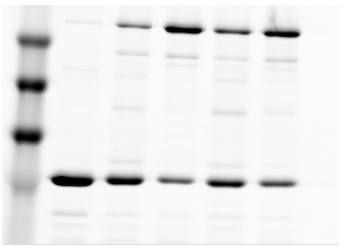

Q223C

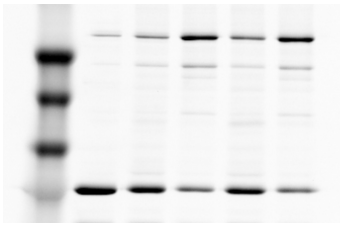

E224C

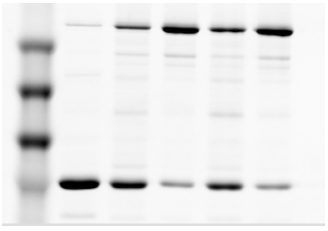

Q225C

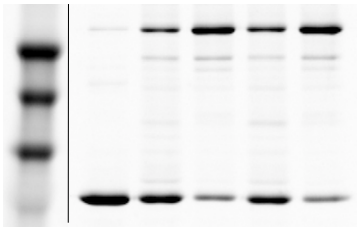

A226C

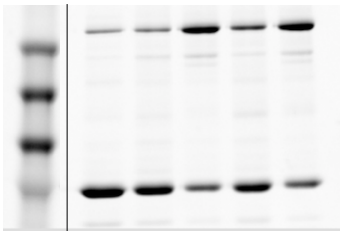

E227C

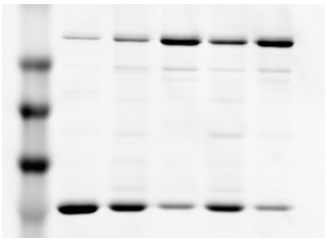

R228C

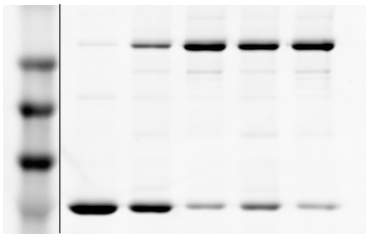

S229C

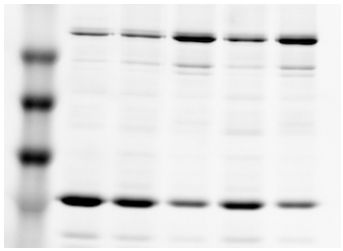

E230C

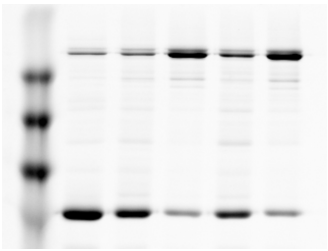

K231C

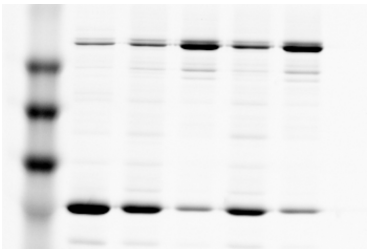

L232C

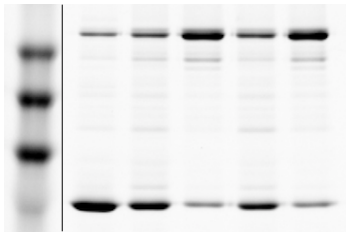

R233C

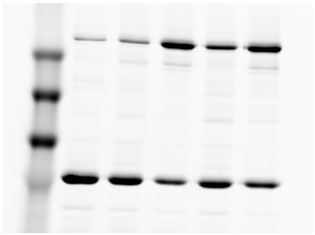

T234C

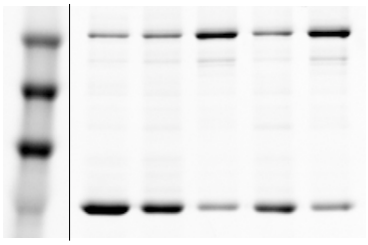

E235C

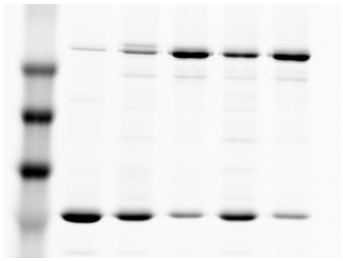

S236C

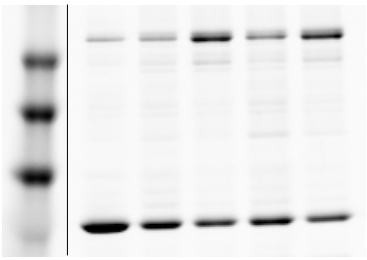

Y237C